1   *Vibrio* elicits targeted transcriptional responses from copepod hosts

2

3   Amalia A. Almada, Ann M. Tarrant#

4

5   Department of Biology, Woods Hole Oceanographic Institution, Woods Hole, Massachusetts,

6   USA

7

8

9   Running head: *Vibrio* elicits transcriptional responses from copepods

10

11

12   # For correspondence. 45 Water Street, Mailstop 33, Woods Hole MA 02543; E-mail
13   atarrant@whoi.edu; Tel. (+1) 508 289 3398; Fax (+1) 508 457 2134.
14

15

16

17

18

19

20

21

22

Abstract:

Copepods are abundant crustaceans that harbor diverse bacterial communities, yet the nature of their interactions with microbiota are poorly understood . Here, we report that *Vibrio* elicits targeted transcriptional responses in the estuarine copepod *Eurytemora affinis*. We pre-treated *E. affinis* with an antibiotic-cocktail and exposed them to either a zooplankton specialist (*Vibrio sp. F10 9ZB36*) or a free-living species (*V. ordalii 12B09*) for 24 hours. We then identified via RNA-Seq a total of 78 genes that were differentially expressed following *Vibrio* exposure, including homologs of C-type lectins, chitin-binding proteins and saposins. The response differed between the two *Vibrio* treatments, with the greatest changes elicited upon inoculation with *V. sp. F10*. We suggest that these differentially regulated genes play important roles in cuticle integrity, the innate immune response, and general stress responses, and that their expression may enable *E. affinis* to recognize and regulate symbiotic vibrios. We further report that *V. sp. F10* culturability is specifically altered upon colonization of *E. affinis*. These findings suggest that rather than acting as passive environmental vectors, copepods discriminately interact with vibrios, which may ultimately impact the abundance and activity of copepod-associated bacteria.

Introduction:

Animals have developed diverse mechanisms to initiate and regulate their interactions with microbiota in order to enrich for specific symbionts and prevent invasion by pathogens within microbially rich environments (Ezenwa *et al.* 2012; Buchon, Broderick and Lemaitre 2013). Those bacteria that successfully associate with hosts receive benefits including increased access to nutrients (Douglas 2009), protection against environmental stressors (Chowdhury *et al.*

46   1997), increased frequency of horizontal gene transfer (Meibom *et al.* 2005; Aminov 2011) and

47   enhanced persistence in the environment (Huq *et al.* 1983). Bacterial communities associated

48   with copepods exhibit increased growth rates and production relative to those bacteria free-living

49   in the surrounding seawater (Griffith, Douglas and Wainright 1990; Carman 1994), in addition to

50   access to unique environments provided by their migrating hosts (Grossart *et al.* 2010).

51   Colonization of copepods by *Vibrio* bacteria is a relatively well-studied zooplankton-bacteria

52   interaction due to the prevalence of pathogenic vibrios (e.g. *V. cholerae*, *V. parahaemolyticus*)

53   on these abundant chitinous organisms (e.g. Huq *et al.* 1983; Rawlings, Ruiz and Colwell 2007)

54   and the dramatic impacts of these associations on the proliferation, virulence and physiology of

55   vibrios (Kirn, Jude and Taylor 2005; Colwell 2009). However, whether copepods are in turn

56   impacted by or further regulate colonizing vibrios is unknown. In light of copepods' abundance

57   across aquatic habitats and enrichment with *Vibrio* associates, copepod physiology may be an

58   important influence on *Vibrio* ecology that has not yet been fully explored.

59   Invertebrate host factors are increasingly recognized for their significant roles in

60   symbiont acquisition and maintenance (Buchon, Broderick and Lemaitre 2013), often

61   contributing to highly host-specific microbiomes (Franzenburg *et al.* 2013). As first lines of

62   defense, the hard, chitinous exoskeleton and gut lining of arthopods such as copepods together

63   form a physical and chemical barrier against pathogen attachment and invasion (Lemaitre and

64   Hoffmann 2007; Vallet-Gely, Lemaitre and Boccard 2008). Chitinous surfaces are also known to

65   induce genetic programs in *Vibrio* species, including the induction of natural competence

66   (Meibom *et al.* 2005). Although invertebrates lack an adaptive immune system, focused studies

67   have revealed a deeper level of complexity of the innate immune system than previously

68   appreciated, including specific immune memory (Kurtz and Franz 2003; Little *et al.* 2003).

69   Elements of the innate immune system, including C-type lectins and antimicrobial peptides

70   (AMPs), are known to enable invertebrate hosts to select for specific bacterial associates in

71   addition to inhibiting growth of undesirable foreigners (Bulgheresi *et al.* 2006; Binggeli *et al.*

72   2014). For example, in the marine nematode *Laxus oneistus,* a mucus-secreted C-type lectin is

73   produced to mediate symbiont association with the cuticle by inducing symbiont aggregation and

74   by directly binding to the symbiont's antigens (Bulgheresi *et al.* 2006). Once bacterial symbionts

75   are acquired, innate immune elements such as AMPs can be crucial for the invertebrate host to

76   further regulate interactions with microbiota, including ensuring the proper localization of the

77   symbionts within the host tissue (Login *et al.* 2011). Such finely-tuned and localized innate

78   immune responses to bacterial symbionts complement those highly conserved, systemic innate

79   immune responses to invading microbes, including the prophenoloxidase (proPO) cascade and

80   catalase activity. The proPO cascade is induced when host recognition proteins are activated by

81   microbial compounds, including bacterial surface attachment proteins and cell wall components

82   (Medzhitov 2007) that initiate the conversion of ProPO into catalytically active phenoloxidase.

83   Phenoloxidase in turn triggers the production of cytotoxic compounds and encapsulation of the

84   microbial invaders (Cerenius, Lee and Söderhäll 2008 and references therein). In addition,

85   catalases enzymatically decompose reactive oxygen species, specifically hydrogen peroxide,

86   which is produced as part of the innate immune response (Ha *et al.* 2005; Wang *et al.* 2013).

87   In this study, we have explored the responses of a copepod host to distinct *Vibrio* species.

88   We chose as our model the copepod *Eurytemora affinis,* an invasive and abundant species that

89   naturally associates with a diversity of pathogenic vibrios (Winkler, Dodson and Lee 2008; Zo *et*

90   *al.* 2009) and has been consistently used in the few laboratory studies examining copepod-*Vibrio*

91   interactions (Huq *et al.* 1983; Huq *et al.* 1984; Rawlings, Ruiz and Colwell 2007). However, to

4

92   our knowledge, our study is the first to examine the potential of the copepod host to

93   discriminately respond to *Vibrio* associations. The two *Vibrio* species tested in this study inhabit

94   similar coastal environments to *E. affinis* (Huq *et al.* 1983; Preheim *et al.* 2011) and possess

95   distinct physical characteristics and ecological specializations: *V. sp. F10* is classified as a

96   zooplankton specialist that lacks the ability to degrade chitin (Preheim 2010; Preheim *et al.*

97   2011), while *V. ordalii* has been inferred to be "almost exclusively free-living" because it is

98   enriched in particle-free fractions of the water column and repeatedly absent from particles,

99   zooplankton, and larger invertebrates (Hunt *et al.* 2008; Preheim *et al.* 2011; Szabo *et al.* 2013).

100   Here, we examined the global transcriptomic response elicited in *E. affinis* by these two

101   ecologically distinct *Vibrio* species.

102

103   **Materials and methods**:

104   ***Vibrio cultures***

105   *Vibrio* growth was first measured over 24 hours to confirm their ability to survive and

106   grow under exposure conditions ideal for *Eurytemora affinis* (i.e. 15 PSU, 18 °C) (Fig. S1). In

107   preparation for *E. affinis* exposure experiments, glycerol stocks of *Vibrio* cultures were streaked

108   onto seawater complete (SWC) agar plates containing 15 PSU artificial seawater (ASW),

109   peptone, yeast extract and glycerol before a 24-hour incubation at room temperature (RT).

110   Several colonies were then transferred into 10 mL of SWC liquid media (15 PSU), shaken at 200

111   rpm and incubated for 19 hours at 18 °C (*V. sp. F10 9ZB36*) or 28 °C (*V. ordalii 12B09;* 28 °C

112   was chosen for *V. ordalii* to ensure robust rapid growth; Fig. S1). For the *E. affinis – Vibrio*

113   exposure experiments, 1 mL of overnight *Vibrio* culture was transferred to 100 mL of SWC

114   liquid media (15 PSU) and incubated for 19 hours at 100 rpm. Cultures were then pelleted at

115   5,500 x g for 5 minutes and rinsed twice with 0.22-μm sterile filtered artificial seawater (15 PSU,

116   RT) before diluting to the desired cell density (2 x 10^7 CFU mL^{-1}). The final dilution factors for

117   each strain were calculated from OD_{600} readings converted to CFU concentrations using

118   independently determined standard curves for each strain and test condition (data not shown).

119   To test whether *V. sp. F10* and *V. ordalii* secrete extracellular chitinases, overnight

120   cultures were grown in SWC media, as described above, spread onto plates comprised of

121   approximately 2% (w/v) colloidal chitin in 1x marine agar (2216), and incubated at room

122   temperature for 24-48 h. Colloidal chitin was prepared from crab shell chitin flakes (Sigma)

123   (Murphy and Bleakeley 2012) and dyed with Remazol Brilliant Violet (Gomez Ramirez *et al.*

124   2004). When extracellular chitinases hydrolyze the chitin substrate and covalently linked dye, a

125   clear halo is left surrounding the chitinase-producing culture. Those cultures that do not secrete

126   chitinases under the conditions examined may grow on the plate but will not produce a clear

127   halo.

128   ***Antibiotic treatment of the estuarine copepod Eurytemora affinis***

129   *Eurytemora affinis* cultures that originated from the Baie de L'isle Verte in the St.

130   Lawrence estuary were generously provided by Carol Lee (University of Wisconsin). The

131   copepod cultures were maintained at 12 °C and 15 PSU on a 14 h light/10 h dark cycle with

132   moderate air bubbling (1-2 bubbles per second). The cultures were fed with *Rhodomonas lens*

133   three times a week at a concentration of 1 x 10^6 cells mL^{-1}.

134   Before *Vibrio* exposure, *E. affinis* were fed and treated for 24 hours with an antibiotic

135   mixture of ampicillin (0.3 mg mL^{-1}), streptomycin (0.1 mg mL^{-1}) and chloramphenicol (0.05 mg

136   mL^{-1}) in moderately aerated, sterile seawater (15 °C, 15 PSU). To initially validate the

137   effectiveness of the antibiotic cocktail in reducing the natural flora of *E. affinis,* individual whole

138   copepods, homogenized copepods, or 400 μL of seawater from flasks containing either antibiotic

139   treated or untreated copepods were placed into 2 mL of marine broth. The absorbance of the

140   marine broth from each of the treatments was measured after 48 hours of incubation at 22 °C. In

141   10 independent experiments, the antibiotic treatment dramatically reduced the OD_{600} of all three

142   sample types (Fig. S2A). In all further *Vibrio* exposure experiments, the effectiveness of the

143   antibiotic treatment was monitored via plate and direct counts of copepods from the control

144   treatments (antibiotic treated and not inoculated with *Vibrio*), as described below, further

145   demonstrating the success of the antibiotic treatment in reducing the native bacterial load (Table

146   1, Fig. S2B, Fig 2C).

E. affinis-Vibrio exposure experiments

148   After 24 h of antibiotic treatment, copepods were rinsed with sterile seawater onto an

149   autoclaved 400-μm sieve and captured with a transfer pipette. In the RNA-Seq experiment, 20

150   mature, adult females were captured for each treatment replicate. 'Mature, adult females' were

151   considered to include ovigerous females and non-ovigerous females with enlarged oviducts full

152   of large oocytes, as previously defined (Boulange-Lecomte, Forget-Leray and Xuereb 2014).

153   Follow-up qPCR experiments were performed with pools (n = 10-20 per replicate) of mature,

154   adult females. For all exposures, copepods were placed into autoclaved 50 mL glass flasks

155   containing *Vibrio* cultures diluted in sterile seawater (15 PSU, 15 °C) and incubated at 18 °C

156   with moderate aeration for 24 h (14 h light/10 h dark cycle). After 24 h of *Vibrio* exposure,

157   copepod samples used for the RNA-Seq and qPCR experiments were gently rinsed onto

158   autoclaved 333-μm mesh, transferred using plastic pipettors into 1 mL of PureZOL (Bio-Rad),

159   and stored at -80 °C until RNA extraction within approximately four weeks.

160   Although the typical density of copepods' natural microbiota is $\sim 10^5$ cells copepod^{-1}

161   within an ambient marine environment containing 10^5-10^6 total bacterial cells mL^{-1} (Möller,

162   Riemann and Sondergaard 2007; Tang, Turk and Grossart 2010), we chose an inoculation

163   density of 2 x 10^7 colony forming units (CFU) mL^{-1} for the RNA-Seq and qPCR expression

164   studies in order to increase the likelihood of eliciting a transcriptomic response in our test

165   animals. Studies examining invertebrate host responses to bacteria frequently use a titre within or

166   above this inoculation density and usually use more direct methods of infection (i.e., injection vs.

167   our approach of immersion, as in Vodovare *et al.* 2005; Watthanasurorot *et al.* 2011; Cha *et al.*

168   2015).

169   To quantify the abundance of bacteria associated with *E. affinis* after 24 h, live copepods

170   from the three treatments (*V. sp. F10*, *V. ordalii*, control) were rinsed onto autoclaved 333-μm

171   mesh sieves with sterile ASW (18 °C, 15 PSU), and whole animals (5 per replicate) were

172   homogenized in 200 μL of filter-sterilized ASW with sterile plastic pestles (Axygen Scientific,

173   #PES15BSI). Homogenized copepods were then serially diluted and incubated for 20 h at RT on

174   seawater complete [SWC] or thiosulfate-citrate-bile salts-sucrose [TCBS] agar plates before

175   counting colony-forming units (CFU). Serial dilutions of the homogenized copepods were also

176   preserved in formalin (1%) and stained with DAPI (10%) for direct counts on 0.22-μm black

177   polycarbonate filters (EMD Millipore Isopore™, GTBP02500) under blue light excitation.

178   Samples from the control treatment were not serially diluted, in anticipation of low cell densities.

179   ***RNA extractions and library sequencing***

180   Total RNA was extracted from *E. affinis* samples using the Aurum Total RNA Fatty and

181   Fibrous Tissue Kit (Bio-Rad). Samples were homogenized in 1 ml PureZOL using a teflon

182   homogenizer and processed according to the manufacturer's protocol, with final elution from

183   columns in 40 μL of warmed elution buffer (Tris buffer), as described previously (Aruda *et al.*

184   2011). For qPCR, residual genomic DNA was removed with on-column DNase digestion. RNA

185   yield and purity were quantified using a Nanodrop ND-1000 spectrophotometer, and RNA

186   quality was visualized on a denaturing agarose gel. Quality of RNA samples submitted for

187   Illumina sequencing was further assessed using a Bioanalyzer. The *E. affinis* samples, like many

188   other arthropods, yielded one sharp peak on the Bioanalyzer due to a hidden break in their 28S

189   rRNA that causes it to run at about the same size as the 18S rRNA.

190   Directional, polyA-enriched RNA libraries were built by the Hudson Alpha Genomic

191   Services Laboratory with the NEBNext® Ultra Directionality Kit (New England BioLabs) from

192   1 μg of total RNA from each sample. The average fragment size of each library was

193   approximately 300 bp. For transcriptome assembly, a library was constructed from a sample of

194   pooled RNA made by combining approximately 200 ng from each sample (4 replicates per

195   control, *V. sp. F10*-exposed, and *V. ordalii*-exposed treatment). The library constructed from this

196   pooled sample was sequenced with 100 bp paired-end reads at a total sequencing depth of 111

197   million reads on a HiSeq 2000. The libraries constructed from each of the twelve individual

198   samples were multiplexed and sequenced across two lanes of the HiSeq2000 with 50 bp paired-

199   end reads at a total depth of 25 million reads per sample for differential expression analysis.

200   ***De novo transcriptome assembly and post-assembly analysis***

9

201   Trimmomatic software (Bolger, Lohse and Usadel 2014) was used in paired-end mode to

202   remove adaptor sequences, low quality sequences (phred score < 20 bp), and the first 12 bp of

203   the 5' end of the read, which often contains a biased nucleotide composition due to nonrandom

204   hexamer priming (Hansen, Brenner and Dudoit 2010). Reads greater than 50 bp in length after

205   quality trimming were retained for assembly, resulting in a total of 102 million reads for

206   assembly. An *E. affinis* transcriptome was assembled *de novo* with the RNA-seq assembler

207   Trinity (version r2013-08-14) using default parameters for paired-end, directional reads

208   (Grabherr *et al.* 2011). The assembled transcriptome consisted of 138,581 contiguous consensus

209   sequences (contigs) that were grouped into 82,891 Trinity components ('genes'). The size range

210   of the transcripts was 201-23,627 bp with an N50 (weighted median) of 2,087 bp. The *E. affinis*

211   assembly is qualitatively similar to other recently reported copepod and amphipod

212   transcriptomes (Table S1). The assembled *E. affinis* transcriptome is accessible through the

213   Transcriptome Shotgun Assembly database (TSA, Bioproject PRJNA242763).

214   Trinity-supported protocols and scripts for downstream analyses were followed using

215   default parameters (Haas *et al.* 2013) to align reads associated with each library to the assembled

216   transcriptome and to estimate abundances of the assembled transcripts (RSEM). Abundance

217   counts of genes were TMM- (trimmed-mean of M-values) and FPKM- (fragments per kilobase

218   per million reads mapped) normalized to account for differences in RNA production across

219   samples (Robinson and Oshlack 2010) and gene length, respectively. The *E. affinis* genome was

220   released in the midst of our analysis (Bioproject PRJNA203087), so a blastn search against the

221   genome with a threshold e-value of 10^{-10} was performed to validate the origin of the transcripts

222   as belonging to *E. affinis*. Principal component analysis (PCA) of the TMM- and FPKM-

223   normalized abundance counts of all biological replicates across the three treatments, with *Vibrio*

224 sequences removed, identified one outlier in the control treatment that was subsequently dropped

225 from further analysis (Fig. S3). Analysis of differentially expressed genes across the three

226 treatments was performed with edgeR software (Robinson, McCarthy and Smyth 2010) with a

227 minimum 2-fold difference in expression and a p-value cutoff for an FDR of 0.05. We chose a 2-

228 fold threshold in light of previous findings that known modulators of host-microbiota

229 interactions are often regulated within this range (Broderick, Buchon and Lemaitre 2014).

230   Representative sequences corresponding to the differentially expressed genes were

231 provisionally annotated using blastx against the NCBI non-redundant (nr) database with a

232 threshold e-value of 10^{-4}. The remainder of the transcriptome was annotated by blastx against the

233 Swissprot database. Blast2GO (Conesa *et al.* 2005) was also used to gain further information

234 about the gene ontology (GO) terms and conserved protein domains associated with the genes of

235 interest.

236 ***Cloning and quantitative PCR (qPCR)***

237   To confirm the predicted sequences of the genes of interest and to generate standards for

238 qPCR, 205-790 bp regions were cloned and sequenced as described previously (Aruda *et al.*

239 2011). All primer sequences are provided in Tables S7 and S8. Material for cloning was

240 obtained from mature, adult *E. affinis* females preserved in PureZOL at -80 °C. Complementary

241 cDNA (cDNA) was synthesized from 1 μg of total RNA per 20 μL reaction using the I-Script

242 cDNA-synthesis kit (Bio-Rad) according to the manufacturer's instructions. PCR products were

243 cloned into pGEM-T Easy (Promega) and sequenced. For qPCR experiments, cDNA was

244 synthesized from 450 ng of total *E. affinis* RNA in a 20 μL reaction. The 20 μL cDNAsynthesis

245 reactions were each diluted with molecular biology grade water, such that each microliter of

246 diluted cDNA corresponded to 10 ng of total RNA.

247 Gene expression was measured using SsoFast EvaGreen Supermix (Bio-Rad) on an

248 iCycler iQ real-time PCR detection system (Bio-Rad). The 20 μL EvaGreen reaction mixture

249 contained 10 μL master mix, 8 μL molecular biology grade water, 1 μL diluted cDNA and 1 μL

250 of 10 μM primers. The PCR conditions were: 95 ^{0}C for 2 min followed by 40 cycles of 95 ^{0}C for

251 5 s and 62 ^{0}C - 64 ^{0}C for 10 s. All samples and standards were run in duplicate wells on the same

252 plate for each gene of interest. After amplification, PCR products from each reaction were

253 subjected to melt-curve analysis to ensure that only a single product was amplified. Selected

254 products were also visualized on agarose gels and consistently yielded single bands.

255 Gene expression was calculated relative to a standard curve of serially diluted plasmid

256 standards encompassing the amplicon of interest and then base-2 log-transformed. A

257 normalization factor equal to the geometric mean of three normalizer genes (Vandesompele *et al.*

258 2002) was subtracted from the gene expression values. The normalizer genes were chosen from

259 the Illumina data based on their moderate expression and low coefficient of variation between

260 samples (i.e., thioredoxin domain-containing protein 5 (comp52262_c0), thyroid adenoma-

261 associated protein homolog (comp59254_c0), and human leucine-rich repeat neuronal protein 2-

262 like (comp53361_c0)). The normalizer genes exhibited stable expression throughout the study

263 except for one *V. sp. F10*-exposed sample that exhibited very low expression of all three

264 normalizer genes and was subsequently removed from further analysis. Results from three

265 independent exposure experiments were combined to give a total of 8 biological replicates (after

266 dropping one *V. sp. F10* replicate, as explained above) in the *V. sp. F10*-exposed treatments, 9

267 replicates in the *V. ordalii*-exposed treatments, and 10 replicates in the control treatment. One-

268   way ANOVAs were used to compare mean gene expression among treatments, except in the

269   cases of C-type lectin-like (comp47544, comp46353, comp49674) and Saposin-like

270   (comp58868) genes, for which Welch ANOVAs were used due to unequal variances among

271   treatments. Unplanned post-hoc comparisons (Tukey's test) in genes with significant ANOVA

272   results ($p < 0.05$) compared all possible pairs of treatment means.

273

274   **Results**:

275   ***Characterization of Vibrio cultures' chitinolytic ability and association with E. affinis***

276   Metabolic characterization of *V. sp. F10 9ZB36* and *V. ordalii 12B09* using colloidal

277   chitin plates suggested that *V. sp. F10* does not secrete exogeneous chitinase under the conditions

278   examined (Fig. S4), in accordance with previous findings that *V. sp. F10* does not metabolize

279   chitin (Preheim 2010). Conversely, *V. ordalii* does appear to secrete chitinase (Fig. S4), although

280   the molecular basis for this physiological difference between the two *Vibrio* species is not clear.

281   We also observed that unlike the copepod-associated *V. ordalii* colonies, the copepod-associated

282   *V. sp. F10* colonies were yellow on TCBS media, suggesting sucrose metabolism.

283   Exposure to *V. sp. F10* did not cause *E. affinis* mortality at any of the inoculation

284   densities tested in this study ($1 - 7 \times 10^7$ CFU mL^{-1}) (Table S2). In some initial experiments,

285   exposure to *V. ordalii* caused low levels of *E. affinis* mortality (5-10%) at inoculation densities

286   of $7 \times 10^6 - 7 \times 10^7$ CFU mL^{-1}. However, no mortalities were observed during any of the

287   inoculations used for the transcriptome and qPCR expression studies (Table S2; densities of $2 \times$

288   10^7 CFU mL^{-1}).We quantified the abundance of bacteria associated with live *E. affinis* in

289   comparison with that of ambient seawater through direct (DAPI staining) and plate counts

290   (*Vibrio*-selective thiosulfate-citrate-bile salts-sucrose [TCBS] and seawater complete [SWC]

291   agar) of whole, homogenized copepods. The direct and plate counts of the copepods from the

292   control treatments (antibiotic-treated, uninoculated) were consistently below statistical limits of

293   detection ($\leq$ 1 cell/field and < 30 CFU/plate, respectively) (Table 1, Fig. 2C, Fig. S2). The

294   copepod-associated bacterial abundances, as measured via direct counts and plate counts on

295   *Vibrio*-selective TCBS media were highly consistent for both *V. ordalii* and *V. sp. F10*

296   treatments (Figure 2).

297   The direct and SWC plate counts of *V. ordalii*-exposed copepods were highly consistent

298   with one another (Fig. 1; Fig. 2; Table 1); conversely, there was great discrepancy (10^6-fold

299   difference) between the direct and SWC plate counts for *V. sp. F10*-exposed copepods across all

300   inoculation titers tested (Fig. 1; Fig. 2; Table 1). The culturability of copepod-associated *V. sp.*

301   *F10* on SWC agar was consistently below detectable levels (< 30 CFU/plate), while direct counts

302   remained high. We observed that the *V. sp. F10* free-living in the ambient seawater of the

303   incubation flasks did not have reduced culturability on SWC agar, suggesting that the change in

304   the *V. sp. F10* culturability is specific to association with copepods (Fig. 2A). The culturability

305   of *V. sp. F10* appears to rapidly decrease upon association with copepods, as there was a 300-

306   fold decrease in culturability on SWC agar between 6 and 24 hours of *E. affinis* inoculation (Fig.

307   S5). Interestingly, copepod-associated *V. sp. F10* demonstrated highly consistent direct and plate

308   counts when the samples were cultured on TCBS agar (Fig. 2A), suggesting that the reduced

309   culturability of copepod-associated *V. sp. F10* is media-specific.

310   ***RNA-Seq differential expression analysis***

14

311   We used RNA-Seq to identify changes in gene expression in *E. affinis* following

312   exposure to either *V. sp. F10* or *V. ordalii*. Overall, relative to the control treatments, the global

313   gene expression pattern of the *V. sp. F10*-exposed treatment was the most distinct (Fig. 3). The

314   global expression pattern of the *V. ordalii*-exposed treatment was very similar to the control

315   treatment (Fig. 3). A total of 78 genes were differentially expressed with a fold change > 2 and a

316   False Discovery Rate (FDR) > 0.05 in pair-wise comparisons of the three treatments (Table S3-

317   S5). The differentially expressed genes were annotated through blastx-based searches of the

318   NCBI nr database, and putative functions were inferred based on associated gene ontology (GO)

319   terms. Among the differentially expressed genes, 38 could be annotated and were associated with

320   diverse predicated functions including cell signaling, immune function, maintenance of cuticle

321   integrity, cellular transport, metabolism, and stress responses (Fig. 4). Many of these functions,

322   notably maintenance of cuticle integrity, immune response, and stress responses, are specifically

323   associated with invertebrate host responses to microbes.

324   The majority of the 78 differentially expressed transcripts originated from the *V. sp. F10*-

325   exposed treatment (61 genes, 47 up-regulated, 14 down-regulated). The genes up-regulated by *V.*

326   *sp. F10* exposure are primarily involved in stress responses, cuticle integrity (chitin metabolism,

327   chitin binding) and the innate immune response (C-type lectins, saposin-like) (Fig. 4, Table S3).

328   *V. sp. F10* exposure also induced mild up-regulation of several cell transport and cell signaling

329   genes, as well as mild down-regulation of several cell signaling, metabolism, stress response and

330   immune elements. Exposure to *V. ordalii* induced few transcriptional changes in *E. affinis*, with

331   strong down-regulation (6-8 fold change compared to control) of two transcripts of unknown

332   function also down-regulated by *V. sp. F10* exposure and mild down-regulation of a knottin-like

333   inhibitory protein unique to the *V. ordalii* exposure treatment (Table S4). A total of 53 genes

334 were differentially expressed between the *V. sp. F10-* and *V. ordalii*-exposed treatments, 16 of

335 which were unique to this comparison (Table S5) and were primarily up-regulated in the *V. sp.*

336 *F10*-exposed treatment. The majority of these genes were of unknown function, with a few

337 involved in cell signaling and maintenance of cuticle integrity (Table S5). Interestingly, two

338 genes were similarly regulated in direction and magnitude in the *V. sp. F10-* and *V. ordalii-*

339 exposed treatments (Fig. 4, Table S5). These two genes had no significant match to the nr or

340 InterProScan databases, although a BLAT (BLAST-like Alignment Tool) search against the *E.*

341 *affinis* genome confirmed their origin as *Eurytemora* (99-100% nucleotide match to *E. affinis*

342 genome; data not shown).

343 ***E. affinis gene expression profiling via qPCR***

344 Eight genes with predicted innate immune function were selected for further qPCR

345 profiling. Six of these genes were differentially expressed within the RNA-Seq study (three C-

346 type lectin-like transcripts, a saposin-like transcript and 2 chitin-binding transcripts). The three

347 C-type lectin-like genes selected for further study are predicted to have mannose-binding

348 domains (Hunter *et al.* 2012) and two of them (comp49674, comp46353) are also predicted to

349 have signal peptides, suggesting they may be secreted (Petersen *et al.* 2011). The saposin-like

350 gene is also predicted to have a signal peptide and to be secreted. Finally, the two chitin-binding

351 genes selected are both predicted to have chitin-binding domains (InterPro), which are often

352 found in genes involved in maintaining the integrity of the arthropod cuticle and gut lining to

353 prevent against invasion of microbes and their toxins (Buchon *et al.* 2009; Kuraishi *et al.* 2011).

354 The RNA-Seq results were strongly supported by the qPCR studies, with consistency in

355 the magnitude and direction of induction of the target genes across the *E. affinis* treatments

356   (Table 1). The three C-type lectin-like and the saposin-like genes were similarly and highly up-

357   regulated across independent *V. sp. F10*-exposed samples (Fig. 5), suggesting tight regulation of

358   these innate immune genes in response to *V. sp. F10* exposure. The chitin-binding genes were

359   more subtly and variably up-regulated in the *V. sp. F10*-exposed treatment (Fig. 5), implying that

360   they may be less tightly regulated than the C-type lectin genes under *V. sp. F10* exposure. Two

361   genes that were not differentially expressed in the transcriptome analysis, prophenoloxidase

362   (proPO) and catalase, were selected for qPCR profiling in light of their highly conserved roles in

363   the innate immune response. In accordance with the RNA-Seq results, proPO and catalase were

364   not differentially expressed upon *Vibrio* exposure via qPCR (Fig. S6).

365

366   **Discussion**:

367   In this study, we investigated the potential of an ecologically significant invertebrate host,

368   the estuarine copepod *E. affinis*, to transcriptionally respond to *Vibrio* exposure. We found that

369   distinct *Vibrio* species elicited discriminate and targeted transcriptional responses in the copepod

370   host and that association with *E. affinis* triggered a change in the culturability of *V. sp. F10*.

371   ***Vibrios elicit distinct transcriptional responses in* E. affinis**

372   The immune response genes up-regulated by *V. sp. F10* association, specifically saposin-

373   like genes and C-type lectins, belong to families that are characteristically involved in symbiont

374   acquisition and maintenance (Bulgheresi *et al.* 2006; Fraune *et al.* 2010; Heath-Heckman *et al.*

375   2014). Saposins can act as pore-forming AMPs in response to microbial infection in a diversity

376   of invertebrates (Banyai and Patthy 1998; Aguilar *et al.* 2005; Roeder *et al.* 2010), while also

377   functioning as selective host regulators of highly stable and specific microbiome communities of

17

378   organisms, including the freshwater cnidarian *Hydra* (Franzenburg *et al.* 2013). In turn,

379   mannose-binding C-type lectins can function as pattern recognition proteins to initiate

380   acquisition of bacterial symbionts from the environment (Bulgheresi *et al.* 2006; Kvennefors *et*

381   *al.* 2008; Bright and Bulgheresi 2010). Additionally, C-type lectins internally inhibit the

382   proliferation of endogenous bacteria by modulating the expression of AMPs (Wang *et al.* 2014)

383   or directly binding to bacteria and acting as antimicrobial agents (Cash *et al.* 2006). Components

384   of highly conserved and systemic innate immune pathways such as the Toll and IMD signaling

385   pathways and the proPO cascade (Franzenburg *et al.* 2013; Binggeli *et al.* 2014; Valenzuela-

386   Munoz and Gallardo-Escarate 2014) were not up-regulated by *V. sp. F10* exposure, highlighting

387   the targeted nature of the immune response elicited by *V. sp. F10*.

388   The mild up-regulation of genes with chitin-binding properties upon *V. sp. F10* exposure

389   may reflect the renewal of the peritrophic membrane to restrict the bacteria from invading the

390   host through the gut (Buchon, Broderick and Lemaitre 2013). A potentially vulnerable point of

391   entry into the host, the gut is lined with the chitinous peritrophic matrix, which acts like a sieve

392   that surrounds and prevents bacteria, bacterial toxins, and hard food fragments from contacting

393   the intestinal epithelium (Lehane 1997). When the thickness and permeability of the peritrophic

394   matrix is compromised in *Drosophila*, there is higher susceptibility to infection by pathogenic

395   bacteria or mortality from bacterial toxins (Kuraishi *et al.* 2011). Furthermore, ingestion of

396   bacteria elicits a stronger immune response in *Drosophila* with a compromised peritrophic

397   matrix, demonstrating the important role that this barrier defense contributes to host immunity

398   (Kuraishi *et al.* 2011). The renewal of the host's chitinous surfaces under an immune response

399   may in turn have significant effects on the physiology of the colonizing vibrios, in light of the

400   dramatic impacts of chitin association on *Vibrio* genetic programs (Kirn, Jude and Taylor 2005;

401   Meibom *et al.* 2005) Further transcriptomic studies could explore whether other naturally

402   associating, chitinolytic vibrios (e.g., *V. cholerae*) trigger stronger up-regulation of chitin-

403   renewal genes in *E. affinis* than do non-chitinolytic zooplankton specialists (i.e., *V. sp. F10*).

404   Exposure to *V. ordalii* induced a limited transcriptomic response in *E. affinis,* despite our

405   observations that *V. ordalii 12B09* can digest chitin and abundantly colonize *E. affinis*. One

406   mildly down-regulated transcript was identified as a knottin-like inhibitory protein, which is

407   commonly involved in the stress and antimicrobial responses of invertebrates (Zhang *et al.*

408   2014). Two of the genes that were strongly down-regulated by *V. ordalii* exposure were

409   similarly down-regulated in the *V. sp. F10* treatment, suggesting that these unknown transcripts

410   may be candidate markers of *Vibrio* exposure (Table S4). Characterization of the function of

411   these two genes and examination of their expression patterns upon copepod exposure to other

412   *Vibrio* species warrant further study. Further examination of the localization of *V. sp. F10* and

413   *V. ordalii* on *E. affinis* via FISH or gfp-labeling could provide important context for the

414   observed differences in the *E. affinis* transcriptomic response to these species, particularly if

415   they are differentially distributed on the internal vs. external "hot spots" of the copepod (i.e.,

416   chitin-lining of the gut and anus vs. mouthparts and carapace) (Sochard *et al.* 1979; Huq *et al.*

417   1983).

418   ***Association with copepods alters culturability of a natural zooplankton specialist***

419   A zooplankton specialist that does not degrade chitin, *V. sp. F10* heavily colonizes *E.*

420   *affinis*. Attachment to *E. affinis* alters the metabolism of *V. sp. F10* by quickly and dramatically

421   reducing its culturability on SWC agar to below detection. This phenomenon is not observed in

422   the free-living *V. sp. F10* collected from the ambient seawater, suggesting that this process is

423   specific to close association with live copepods and is not likely caused by a broadly secreted

424   factor. The association of bacteria that are non-culturable on standard media but are detectable

425   by immunological or PCR-based methods (i.e., viable but non-culturable, VBNC) with copepods

426   and other zooplankton has been frequently observed in environmental samples (Huq *et al.* 1983;

427   Signoretto *et al.* 2005; Thomas *et al.* 2006). The VBNC phenomenon is thought to enhance

428   bacterial survival during unfavorable environmental conditions, including dramatic shifts in

429   salinity and temperature (Colwell 2009).

430   Many previous studies describe VBNC vibrios as non-culturable on TCBS agar

431   (Chowdhury *et al.* 1997; Signoretto *et al.* 2005; Halpern *et al.* 2007), a highly selective medium

432   often used for isolation and enumeration of vibrios. In contrast, we found that the *V. sp. F10*

433   associated with copepods are culturable on TCBS agar but non-culturable on SWC agar. Further

434   study is needed to identify which components unique to TCBS media, including sucrose and bile

435   salts, lead to the observed differences in the culturability of copepod-associated *V. sp. F10* on

436   SWC and TCBS agar plates. Even upon entering the VBNC state, *Vibrio* species can be highly

437   sensitive to bile salts (Su, Jane and Wong 2013), which are known to affect the physiology of

438   many bacteria (Begley, Gahan and Hill 2005) and can serve as stimuli for biofilm formation,

439   increased motility, and activation of virulence genes in *Vibrio* (Hung *et al.* 2006; Gotoh *et al.*

440   2010; Hay and Zhu 2014). In light of *V. sp. F10*'s strong association with living zooplankton in

441   the natural environment (Preheim *et al.* 2011), future work should also investigate whether

442   physiological changes associated with altered culturability of copepod-associated *V. sp. F10*

443   confer a fitness advantage to *V. sp. F10*.

444   To conclude, our study demonstrates that the estuarine copepod *E. affinis* dynamically

445   and discriminately interacts with *Vibrio* species. Specifically, we have shown that *E. affinis* can

446   distinctly respond to *Vibrio* through targeted up-regulation of immune elements that may be

447   involved in the recognition and maintenance of symbiotic *Vibrio* associates. The effect of *E.*

448   *affinis* association on *V. sp. F10* culturability highlights our limited understanding of the impacts

449   of copepod association on vibrios. We propose that continued study of the dynamics of copepod-

450   *Vibrio* interactions may reveal that copepod physiology is a significant influence on *Vibrio*

451   activity and abundance in the natural environment.

452

472

473

474   **References:**

475   Aguilar R, Jedlicka AE, Mintz M, *et al.* Global gene expression analysis of *Anopheles gambiae*
476   responses to microbial challenge. *Insect Biochem Mol Biol* 2005;**35**:709-19.
477   Aminov RI Horizontal gene exchange in environmental microbiota. *Frontiers in Microbiology*
478   2011;**2**:158.
479   Aruda AM, Baumgartner MF, Reitzel AM, *et al.* Heat shock protein expression during stress and
480   diapause in the marine copepod *Calanus finmarchicus*. *J Insect Physiol* 2011;**57**:665-75.
481   Banyai L, Patthy L Amoebapore homologs of *Caenohabditis elegans*. *Biochim Biophys Acta*
482   1998;**1429**:259-64.
483   Begley M, Gahan CGM, Hill C The interaction between bacteria and bile. *FEMS Microbiol Rev*
484   2005;**29**:625-51.
485   Binggeli O, Neyen C, Poidevin M, *et al.* Prophenoloxidase activation is required for survival to
486   microbial infections in *Drosophila*. *PLoS Pathogens* 2014;**10**:e1004067.
487   Bolger AM, Lohse M, Usadel B Trimmomatic: a flexible trimmer for Illumina sequence data.
488   *Bioinformatics* 2014;**30**:2114-20.
489   Boulange-Lecomte C, Forget-Leray J, Xuereb B Sexual dimorphism in Grp78 and Hsp90A heat
490   shock protein expression in the estuarine copepod *Eurytemora affinis*. *Cell Stress Chaperones*
491   2014;**19**:591-7.
492   Bright M, Bulgheresi S A complex journey: transmission of microbial symbionts. *Nature Rev*
493   *Microbiol* 2010;**8**:218-30.
494   Broderick NA, Buchon N, Lemaitre B Microbiota-induced changes in *Drosophila melanogaster*
495   host gene expression and gut morphology. *mBio* (2014);**5**:10.1128/mBio.01117-14
496   Buchon N, Broderick NA, Lemaitre B Gut homeostasis in a microbial world: insights from
497   *Drosophila melanogaster*. *Nature Rev Microbiol* 2013;**11**:615-26.
498   Buchon N, Broderick NA, Poidevin M, *et al. Drosophila* intestinal response to bacterial
499   infection: activation of host defense and stem cell proliferation. *Cell Host Microbe* 2009;**5**:200-
500   11.

Bulgheresi S, Schabussova I, Chen T, *et al.* A new C-type lectin similar to the human immunoreceptor DC-SIGN mediates symbiont acquisition by a marine nematode. *Appl Environ Microbiol* 2006;**72**:2950-6.

Carman KR Stimulation of marine free-living and epibiotic bacterial activity by copepod excretions. *FEMS Microbiol Ecol* 1994;**14**:255-61.

Cash HL, Whitham CV, Behrendt CL, *et al.* Symbiotic bacteria direct expression of an intestinal bactericidal lectin. *Science* 2006;**313**:1126-30.

Cerenius L, Lee BL, Söderhäll K The proPO-system: pros and cons for its role in invertebrate immunity. *Trends Immunol* 2008;**29**:263-71.

Cha G-H, Liu Y, Peng T, *et al.* Molecular cloning, expression of a galectin gene in Pacific white shrimp *Litopenaeus vannamei* and the antibacterial activity of its recombinant protein. *Molecular Immunology* 2015;**67**:325-40.

Chowdhury MAR, Huq A, Xu B, *et al.* Effect of alum on free-living and copepod-associated *Vibrio cholerae* O1 and O139. *Appl Environ Microbiol* 1997;**63**:3323-6.

Colwell RR Viable but not cultivable bacteria. In: Epstein SS (ed.). *Uncultivated Microorganisms,*Springer Berlin Heidelberg, 2009,**10:**121-9.

Conesa A, Gotz S, Garcia-Gomez JM, *et al.* Blast2GO: a universal tool for annotation, visualization and analysis in functional genomics research. *Bioinformatics* 2005;**21**:3674-6.

Douglas AE The microbial dimension in insect nutritional ecology. *Funct Ecol* 2009;**23**:38-47.

Ezenwa VO, Gerardo NM, Inouye DW, *et al.* Animal behavior and the microbiome. *Science* 2012;**338**:198-9.

Franzenburg S, Walter J, Künzel S, *et al.* Distinct antimicrobial peptide expression determines host species-specific bacterial associations. *Proc Nat Acad Sci USA* 2013;**110**:E3730-E8.

Fraune S, Augustin R, Anton-Erxleben F, *et al.* In an early branching metazoan, bacterial colonization of the embryo is controlled by maternal antimicrobial peptides. *Proc Nat Acad Sci USA* 2010;**107**:18067-72.

Gomez Ramirez M, Rojas Avelizapa LI, Rojas Avelizapa NG, *et al.* Colloidal chitin stained with Remazol Brilliant Blue, a useful substrate to select chitinolytic microorganisms and to evaluate chitinases. *J Microbiol Methods* 2004;**56**:213-9.

Gotoh K, Kodama T, Hiyoshi H, *et al.* Bile acid-induced virulence gene expression of *Vibrio parahaemolyticus* reveals a novel therapeutic potential for bile acid sequestrants. *PLoS ONE* 2010;**5**:e13365.

Grabherr MG, Haas BJ, Yassour M, *et al.* Full-length transcriptome assembly from RNA-Seq data without a reference genome. *Nature Biotechnol* 2011;**29**:644-52.

Griffith PC, Douglas DJ, Wainright SC Metabolic activity of size-fractionated microbial plankton in estuarine, nearshore, and continental shelf waters of Georgia. *Mar Ecol Prog Ser* 1990;**59**:263-70.

Grossart HP, Dziallas C, Leuner F, *et al.* Bacterial dispersal by hitchhiking on zooplankton. *Proc Nat Acad Sci USA* 2010;**107**:11959-64.

Ha E-M, Oh C-T, Ryu J-H, *et al.* An antioxidant system required for host protection against gut infection in *Drosophila*. *Dev Cell* 2005;**8**:125-32.

Haas BJ, Papanicolaou A, Yassour M, *et al.* De novo transcript sequence reconstruction from RNA-seq using the Trinity platform for reference generation and analysis. *Nature Protocols* 2013;**8**:1494-512.

Halpern M, Landsberg O, Raats D, *et al.* Culturable and VBNC *Vibrio cholerae*: interactions with chironomid egg masses and their bacterial population. *Microbial Ecol* 2007;**53**:285-93.

547 Hansen KD, Brenner SE, Dudoit S Biases in Illumina transcriptome sequencing caused by
548 random hexamer priming. *Nucleic Acids Res* 2010;**38**:e131.
549 Hay AJ, Zhu J Host intestinal signal-promoted biofilm dispersal induces *Vibrio cholerae*
550 colonization. *Infection and Immunity* 2014;IAI.02617-14.
551 Heath-Heckman EA, Gillette AA, Augustin R, *et al.* Shaping the microenvironment: evidence
552 for the influence of a host galaxin on symbiont acquisition and maintenance in the squid-vibrio
553 symbiosis. *Environ Microbiology* 2014;**16**:3669-82.
554 Hung DT, Zhu J, Sturtevant D, *et al.* Bile acids stimulate biofilm formation in *Vibrio cholerae*.
555 *Mol Microbiol* 2006;**59**:193-201.
556 Hunt DE, David LA, Gevers D, *et al.* Resource partitioning and sympatric differentiation among
557 closely related bacterioplankton. *Science* 2008;**320**:1081-5.
558 Hunter S, Jones P, Mitchell A, *et al.* InterPro in 2011: new developments in the family and
559 domain prediction database. *Nucleic Acids Res* 2012;**40**:16.
560 Huq A, West PA, Small EB, *et al.* Influence of water temperature, salinity, and pH on survival
561 and growth of toxigenic *Vibrio cholerae* serovar 01 associated with live copepods in laboratory
562 microcosms. *Appl Environ Microbiol* 1984;**48**:420-4.
563 Huq A, Small EB, West PA, *et al.* Ecological relationships between *Vibrio cholerae* and
564 planktonic crustacean copepods. *Appl Environ Microbiol* 1983;**45**:275-83.
565 Kirn TJ, Jude BA, Taylor RK A colonization factor links *Vibrio cholerae* environmental survival
566 and human infection. *Nature* 2005;**438**:863-6.
567 Kuraishi T, Binggeli O, Opota O, *et al.* Genetic evidence for a protective role of the peritrophic
568 matrix against intestinal bacterial infection in *Drosophila melanogaster*. *Proc Nat Acad Sci USA*
569 2011;**108**:15966-71.
570 Kurtz J, Franz K Innate defence: evidence for memory in invertebrate immunity. *Nature*
571 2003;**425**:37-8.
572 Kvennefors ECE, Leggat W, Hoegh-Guldberg O, *et al.* An ancient and variable mannose-binding
573 lectin from the coral *Acropora millepora* binds both pathogens and symbionts. *Dev Comp*
574 *Immunol* 2008;**32**:1582-92.
575 Lehane MJ Peritrophic matrix structure and function. *Ann Rev Entemol* 1997;**42**:525-50.
576 Lemaitre B, Hoffmann J The host defense of *Drosophila melanogaster*. *Ann Rev Immunol*
577 2007;**25**:697-743.
578 Little TJ, O'Connor B, Colegrave N, *et al.* Maternal transfer of strain-specific immunity in an
579 invertebrate. *Curr Biol* 2003;**13**:489-92.
580 Login FH, Balmand S, Vallier A, *et al.* Antimicrobial peptides keep insect endosymbionts under
581 control. *Science* 2011;**334**:362-5.
582 Medzhitov R Recognition of microorganisms and activation of the immune response. *Nature*
583 2007;**449**:819-26.
584 Meibom KL, Blokesch M, Dolganov NA, *et al.* Chitin induces natural competence in *Vibrio*
585 *cholerae*. *Science* 2005;**310**.
586 Möller EF, Riemann L, Sondergaard M Bacteria associated with copepods: abundance, activity
587 and community composition. *Aquat Microb Ecol* 2007;**47**:99-106.
588 Murphy N, Bleakeley B Simplified method of preparing colloidal chitin used for screening of
589 chitinase-producing microorganisms. *Internet J Microbiol* 2012;**10**:2.
590 Petersen TN, Brunak S, von Heijne G, *et al.* SignalP 4.0: discriminating signal peptides from
591 transmembrane regions. *Nature Methods* 2011;**8**:785-6.

592 Preheim SP Ecology and population structure of *Vibrionaceae* in the coastal ocean. 2010; Ph.D.
593 Thesis, Massachusetts Institute of Technology, Cambridge Massachusetts.
594 Preheim SP, Boucher Y, Wildschutte H, *et al.* Metapopulation structure of *Vibrionaceae* among
595 coastal marine invertebrates. *Environ Microbiol* 2011;**13**:265-75.
596 Rawlings TK, Ruiz GM, Colwell RR Association of *Vibrio cholerae* O1 El Tor and O139
597 Bengal with the copepods *Acartia tonsa* and *Eurytemora affinis*. *Appl Environ Microbiol*
598 2007;**73**:7926-33.
599 Robinson MD, Oshlack A A scaling normalization method for differential expression analysis of
600 RNA-seq data. *Genome Biol* 2010;**11**:R25.
601 Robinson MD, McCarthy DJ, Smyth GK edgeR: a Bioconductor package for differential
602 expression analysis of digital gene expression data. *Bioinformatics* 2010;**26**:139-40.
603 Roeder T, Stanisak M, Gelhaus C, *et al.* Caenopores are antimicrobial peptides in the nematode
604 *Caenorhabditis elegans* instrumental in nutrition and immunity. *Dev Comp Immunol*
605 2010;**34**:203-9.
606 Signoretto C, Burlacchini G, Pruzzo C, *et al.* Persistence of *Enterococcus faecalis* in aquatic
607 environments via surface interactions with copepods. *Appl Environ Microbiol* 2005;**71**:2756-61.
608 Sochard MR, Wilson DF, Austin B, *et al.* Bacteria associated with the surface and gut of marine
609 copepods. *Appl Environ Microbiol* 1979;**37**:750-9.
610 Su C-P, Jane W-N, Wong H-c Changes of ultrastructure and stress tolerance of *Vibrio*
611 *parahaemolyticus* upon entering viable but nonculturable state. *Int J Food Microbiol*
612 2013;**160**:360-6.
613 Szabo G, Preheim SP, Kauffman KM, *et al.* Reproducibility of *Vibrionaceae* population
614 structure in coastal bacterioplankton. *ISME J* 2013;**7**:509-19.
615 Tang KW, Turk V, Grossart H-P Linkage between crustacean zooplankton and aquatic bacteria.
616 *Aquat Microb Ecol* 2010;**61**:261-77.
617 Thomas KU, Joseph N, Raveendran O, *et al.* Salinity-induced survival strategy of *Vibrio*
618 *cholerae* associated with copepods in Cochin backwaters. *Mar Pollut Bull* 2006;**52**:1425-30.
619 Valenzuela-Munoz V, Gallardo-Escarate C TLR and IMD signaling pathways from *Caligus*
620 *rogercresseyi* (Crustacea: Copepoda): In silico gene expression and SNPs discovery. *Fish*
621 *Shellfish Immunol* 2014;**36**:428-34.
622 Vallet-Gely I, Lemaitre B, Boccard F Bacterial strategies to overcome insect defenses. *Nature*
623 *reviews Microbiology* 2008;**6**:302-13.
624 Vandesompele J, De Preter K, Pattyn F, *et al.* Accurate normalization of real-time quantitative
625 RT-PCR data by geometric averaging of multiple internal control genes. *Genome Biol*
626 2002;**3**:E0034.
627 Vodovare N, Vinals M, Liehl P, *et al. Drosophila* host defense after oral infection by an
628 entomopathogenic *Pseudomonas* species. *Proc Nat Acad Sci USA* 2005;**102**.
629 Wang C, Yue X, Lu X, *et al.* The role of catalase in the immune response to oxidative stress and
630 pathogen challenge in the clam *Meretrix meretrix*. *Fish Shellfish Immunol* 2013;**34**:91-9.
631 Wang X-W, Xu J-D, Zhao X-F, *et al.* A shrimp C-type lectin inhibits proliferation of the
632 hemolymph microbiota by maintaining the expression of antimicrobial peptides. *J Biol Chem*
633 2014;**289**:11779-90.
634 Watthanasurorot A, Jiravanichpaisal P, Liu H, *et al.* Bacteria-induced Dscam isoforms of the
635 crustacean, *Pacifastacus leniusculus*. *PLoS Pathog* 2011;**7**:e1002062.

636 Winkler G, Dodson JJ, Lee CE Heterogeneity within the native range: population genetic
637 analyses of sympatric invasive and noninvasive clades of the freshwater invading copepod
638 *Eurytemora affinis*. *Molecular Ecology* 2008;**17**:415-30.
639 Zhang C-R, Zhang S, Xia J, *et al.* The immune strategy and stress response of the Mediterranean
640 species of the *Bemisia tabaci* complex to an orally delivered bacterial pathogen. *PLoS ONE*
641 2014;**9**:e94477.
642 Zo Y-G, Chokesajjawatee N, Grim C, *et al.* Diversity and seasonality of bioluminescent *Vibrio*
643 *cholerae* populations in Chesapeake Bay. *Appl Environ Microbiol* 2009;**75**:135-46.

644

645

646

647

Figure and legends:

Fig. 1. Association with the copepod *E. affinis* reduces *Vibrio sp. F10* culturability on seawater complete agar across a range of inoculation densities. *V. sp. F10* (A) and *V. ordalii* (B) isolated from pools (n = 5) of homogenized adult, mature female *E. affinis* were either directly stained with DAPI (asterisks) or plated on seawater complete (SWC) agar (circles) and incubated at room temperature for 20 hours. Abundances are plotted as the base-10 log-transformed means of two biological replicates. Error bars indicate standard error and frequently fall within the area of the symbol. Note that the symbols associated with the direct and plate counts for *V. ordalii* lie on top of one another. The direct and plate counts of the copepods from the control treatments are not shown because they were consistently below detection (≤ 1 cell/field and < 30 CFU/plate, respectively).

Fig. 2. Reduction of *Vibrio sp. F10* culturability upon colonization of the *E. affinis* surface is media-specific. Equivalent bacterial concentration of antibiotic pre-treated copepods 24 hours after inoculation with a bacterial density of 2×10^7 CFU mL^{-1} *V. sp. F10* (A), *V. ordalii* (B), or no bacterial inoculation control (C). Bacteria isolated from pools (n = 5) of homogenized adult, mature female *E. affinis* or from the ambient seawater were either directly stained with DAPI (asterisks), plated on seawater complete (SWC) agar (circles), or plated on thiosulfate-citrate-bile salts-sucrose (TCBS) agar (triangles) and incubated at room temperature for 20 hours. Equivalent concentration of copepod-associated bacteria was calculated by dividing counts per copepod by the approximate volume of *E. affinis* ($\sim 2.5 \times 10^{-5}$ mL) to qualitatively compare ambient seawater and copepod-associated bacterial concentrations (Tang *et al.* 2010). SWC plate counts of *V. sp. F10* isolated from *E. affinis* were consistently below the statistical detection limit (< 30 CFU/plate) and therefore were not normalized to *E. affinis* body volume. The direct

and plate counts of the copepods from the control treatments were consistently below detection (≤ 1 cell/field and < 30 CFU/plate, respectively). All counts were base-10 log-transformed and replicates were jittered along the x-axis to improve readability. In the control panel (C), all negative log-transformed values and zero counts (undefined log value) were replaced with a zero for ease of presentation.

Fig. 3. *Vibrio* species elicit distinct transcriptional profiles in *E. affinis*. (Left) Principal component analysis demonstrates strong distinction between the *V. sp. F10*-exposed and control treatments, with little distinction between the *V. ordalii*-exposed and control treatments. (Right) A heat map representing the base-2 log-transformed FPKM expression values of the 78 differentially expressed genes (fold change > 2, FDR > 0.05) across the three *Vibrio* exposure treatments demonstrates a similar trend. Colors to the left of the heat map represent clades of transcripts with similar expression patterns Horizontal groupings indicate hierarchical clustering of biological replicates by global transcript expression patterns.

Fig. 4. *Vibrio* exposure alters expression of genes putatively involved in invertebrate host response to microbiota. (Left) Functional gene ontology terms associated with the 78 differentially expressed genes identified by Illumina sequencing. The total gene number in each category is indicated on the pie chart. (Right) Highlight of *E. affinis* genes that were most altered by exposure to *Vibrio*. Base-2 log-transformed fold changes ($\log_2$FC) in gene expression for each *Vibrio* exposure condition are relative to the control treatment. Positive and negative $\log_2$FC values reflect genes up-regulated and down-regulated, respectively, compared to the control treatment. Genes highlighted with bolder colors are more intensely altered by *Vibrio* exposure,

with red hues indicating up-regulation and blue hues indicating down-regulation. Those genes further profiled by qPCR are in bold.

Fig. 5. qPCR validation of RNA-Seq gene targets up-regulated upon *V. sp. F10* exposure. Gene expression was measured in pooled samples of adult female *E. affinis* (n = 10-20 individuals), and results from three independent *Vibrio* exposure experiments were pooled for a for a total of n = 10, 9, 8 biological replicates in the control, *V. ordalii*, and *V. sp. F10* treatments, respectively. Expression values were normalized to housekeeping genes and base-2 log-transformed. The F-statistics ('F(W)') and p-values from Welch ANOVAs are listed for each profiled gene. Tukey's post-hoc comparisons demonstrated that the *V. sp. F10* treatment, labelled and indicated in red, was significantly different from the *V. ordalii* and control treatments in each of the genes profiled here.

Table 1: Abundance of bacteria associated with the estuarine copepod *Eurytemora affinis* after 24 hours of exposure.
After 24 h of antibiotic pre-treatment, inoculation with *Vibrio* culture or seawater (control), and 24 h of incubation (18 °C, 15 PSU), whole live copepods (5 per replicate) were rinsed with artificial seawater, homogenized, and stained with DAPI or plated on seawater complete agar (15 PSU) to obtain direct and plate (culturable) counts, respectively. Counts are listed as means ± standard error of two biological replicates. 'Density of total bacteria' attached to control copepods are not listed because the direct counts of these samples were consistently below detection (≤ 1 cell/field). [a]Indicates the culturable bacteria counts are approximate because they are below the statistical detection limit (< 30 CFU/plate). [b]Indicates there is one biological replicate.

| *Vibrio* strain	Inoculation density (CFU mL^{-1})	Density of culturable bacteria attached to copepods (CFU/copepod)	Density of total bacteria attached to copepods (direct cell counts/copepod)	Density of culturable bacteria on controls (CFU/copepod)	Sex of copepods in experiment
V. sp. F10 9ZB36	1.0×10^7	0 ± 0 [a]	$2.3 \times 10^6 \pm 4.0 \times 10^5$	0.6 ± 0.6	Males and females (>400 μm)
V. sp. F10 9ZB36	2.0×10^7	18.5 ± 1.5 [a]	$2.0 \times 10^6 \pm 5.0 \times 10^5$	2.5 ± 1	Mature, adult females
V. sp. F10 9ZB36	2.0×10^7	4.9 ± 1.1 [a]	$7.4 \times 10^5 \pm 2.7 \times 10^5$	8.5 ± 1	Mature, adult females
V. sp. F10 9ZB36	2.0×10^7	15.6 ± 9.9 [a]	$5.0 \times 10^6 \pm 1.1 \times 10^6$	0.75 ± 0.25	Mature, adult females
V. sp. F10 9ZB36	2.5×10^7	0 ± 0 [a]	1.2×10^6 [b]	0 ± 0	Males and females (>400 μm)
V. sp. F10 9ZB36	6.0×10^7	6.0 ± 2.0 [a]	-	0.75 ± 0.75	Mature, adult females
V. ordalii 12B09	6.0×10^6	$2.1 \times 10^3 \pm 6.0 \times 10^2$	-	0.2 ± 0.2	Males and females (>400 μm)
V. ordalii 12B09	7.0×10^6	7.0×10^3 [b]	-	2.8 ± 0.4	Males and females (>400 μm)
V. ordalii 12B09	2.0×10^7	$2.7 \times 10^4 \pm 9.0 \times 10^3$	$3.1 \times 10^4 \pm 4.5 \times 10^3$	2.5 ± 1	Mature, adult females
V. ordalii 12B09	2.0×10^7	$3.2 \times 10^4 \pm 1.4 \times 10^4$	$4.9 \times 10^4 \pm 3.5 \times 10^3$	8.5 ± 1	Mature, adult females
V. ordalii 12B09	2.0×10^7	9.0×10^4 [a, b]	3.1×10^4 [b]	0 ± 0	Mature, adult females
V. ordalii 12B09	2.0×10^7	$1.4 \times 10^4 \pm 6.0 \times 10^3$	$1.6 \times 10^5 \pm 1.5 \times 10^4$	0.75 ± 0.25	Mature, adult females
V. ordalii 12B09	3.0×10^7	$2.0 \times 10^4 \pm 1.0 \times 10^4$	$3.3 \times 10^4 \pm 8.5 \times 10^3$	1.25 ± 0.75	Males and females (>400 μm)
V. ordalii 12B09	6.0×10^7	$3.4 \times 10^4 \pm 2.0 \times 10^3$	$2.0 \times 10^5 \pm 2.0 \times 10^4$	0.2 ± 0.2	Males and females (>400 μm)
V. ordalii 12B09	6.0×10^7	$4.4 \times 10^4 \pm 1.0 \times 10^3$	-	0.75 ± 0.75	Mature, adult females
V. ordalii 12B09	6.0×10^7	$5.4 \times 10^4 \pm 2.5 \times 10^3$	-	0 ± 0	Mature, adult females
V. ordalii 12B09	7.0×10^7	$1.2 \times 10^5 \pm 6.1 \times 10^4$	$2.0 \times 10^4 \pm 2.5 \times 10^4$	2.8 ± 0.4	Males and females (>400 μm)

A. *V. sp. F10*
○ SWC Plate Counts
✳ Direct Counts

B. *V. ordalii*
○ SWC Plate Counts
✳ Direct Counts

Fig 1

A. and B. x-axis: **Inoculation Density (x 10^7 CFU ml^{-1})**

A. and B. y-axis: **Log Counts Copepod^{-1}**

Fig 2

Fig 3

Fig 4

5

10

40

6

4

8

5

■ Transport
■ Signaling
■ Cuticle integrity
■ Stress response
□ Immune response
■ Metabolism
■ Unknown
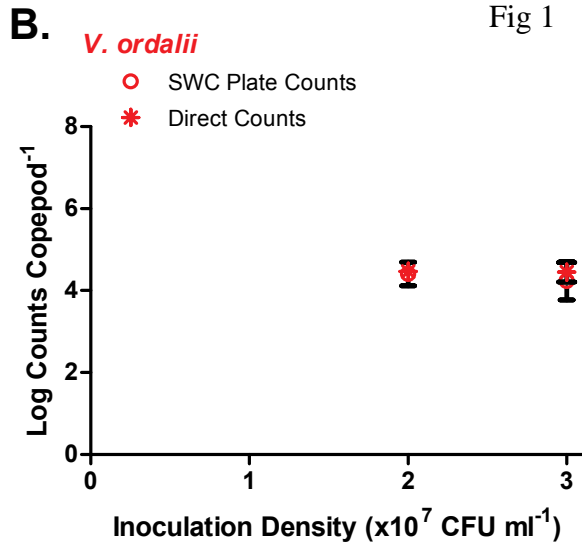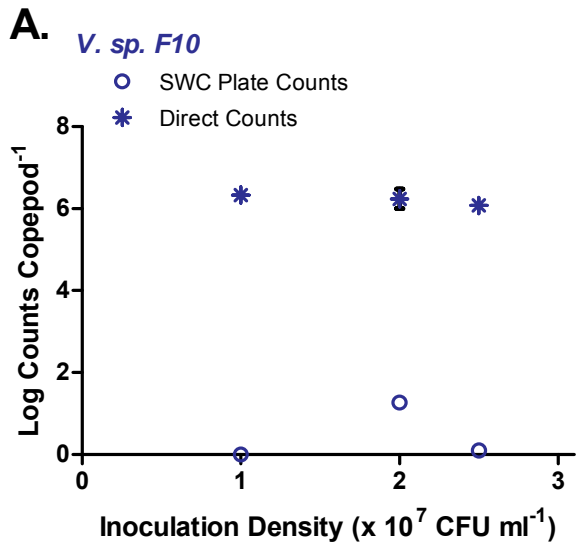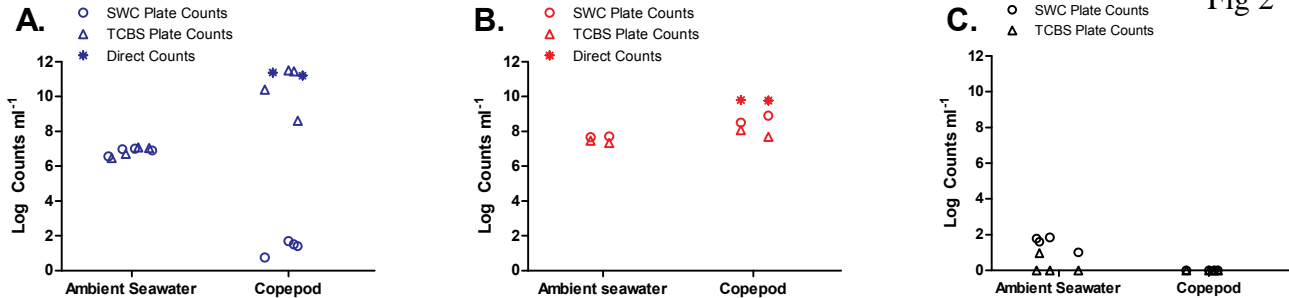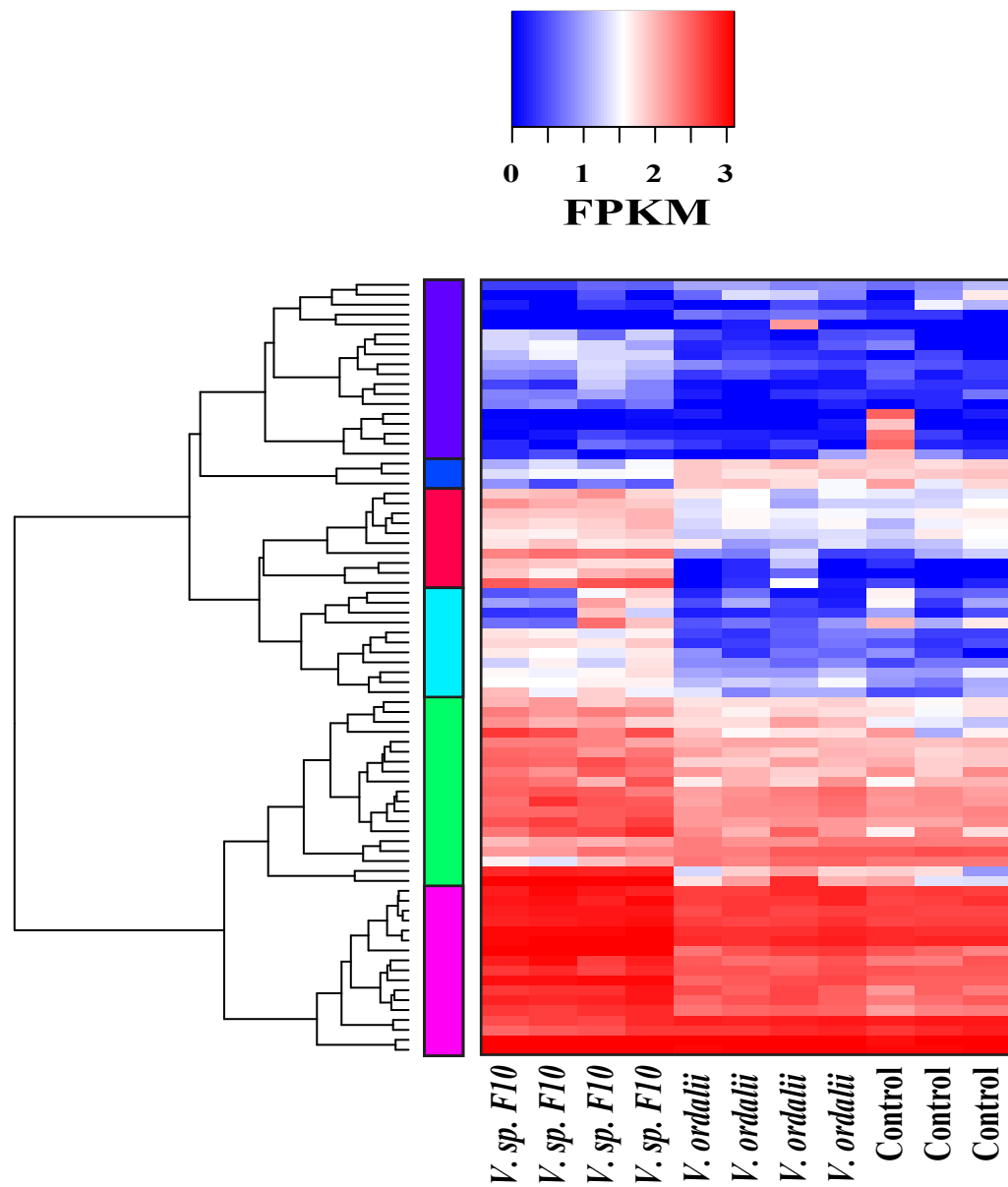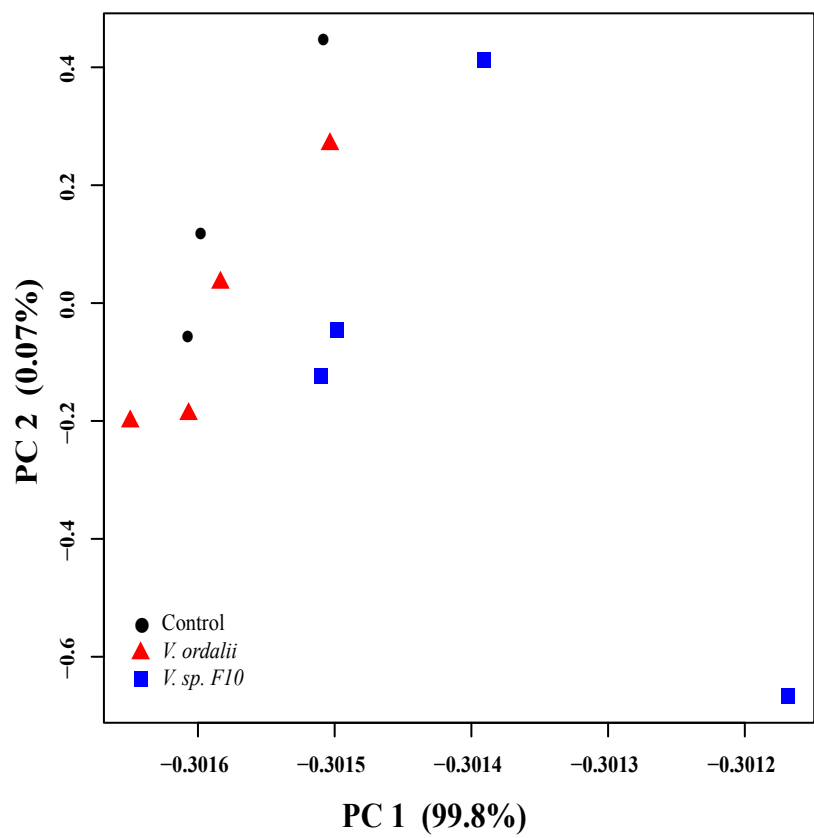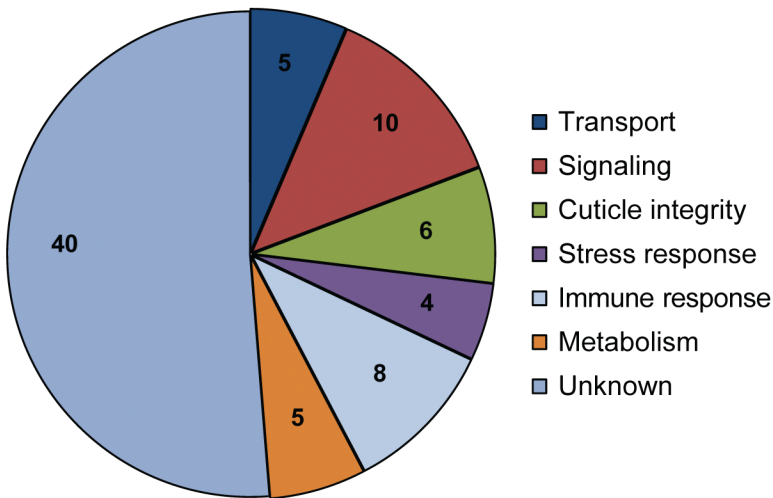
Function	Transcript ID	log$_2$FC (*V. sp. F10*)	log$_2$FC (*V. ordalii*)
RESPONSE TO STRESS			
Injury response	comp32809_c1	1.59	-
Detoxification	comp55690_c0	-1.50	-
Detoxification	comp46208_c1	-1.04	-
Inhibitory protein	comp44575_c0	-	-2.81
CUTICLE INTEGRITY			
Chitin metabolism	comp55805_c0	1.28	-
Chitin-binding	comp35157_c0	1.88	-
Chitin-binding	**comp43891_c0**	2.10	-
Chitin-binding	**comp47090_c0**	2.03	-
IMMUNE SYSTEM PROCESSES			
C-type lectin-like	comp43463_c0	-1.16	-
C-type lectin-like	comp50187_c1	-1.80	-
Saposin-like	**comp58868_c1**	4.52	-
C-type lectin-like	comp46353_c0	8.21	-
C-type lectin-like	**comp46353_c1**	7.64	-
C-type lectin-like	**comp49674_c0**	6.93	-
C-type lectin-like	**comp47544_c0**	4.61	-
C-type lectin-like	comp40027_c0	5.99	-
UNKNOWN			
Unknown	comp51822_c0	-5.53	-5.90
Unknown	comp40339_c0	-8.35	-7.66

Fig 5

A

B
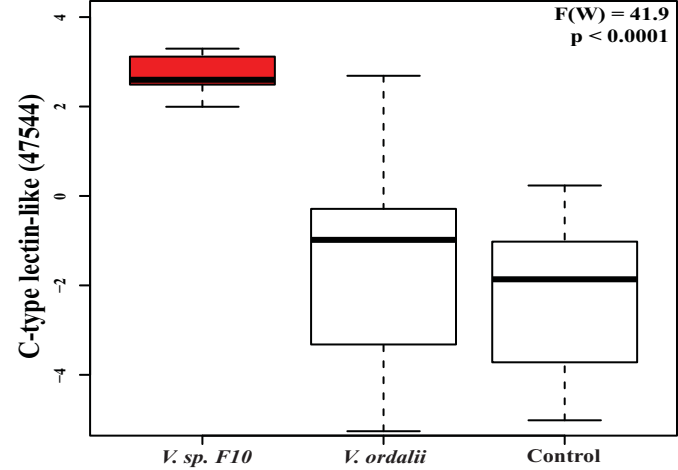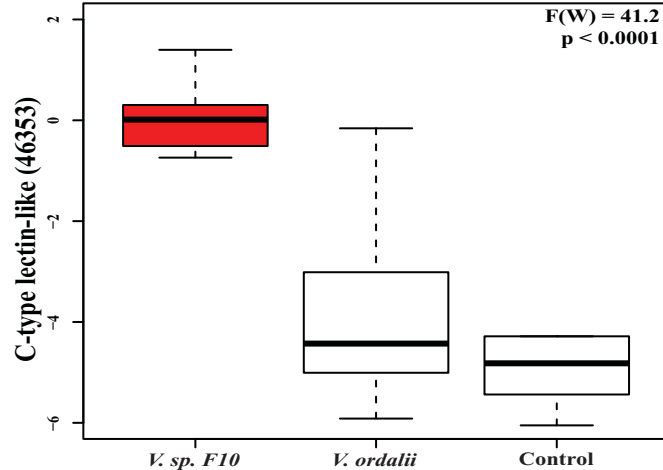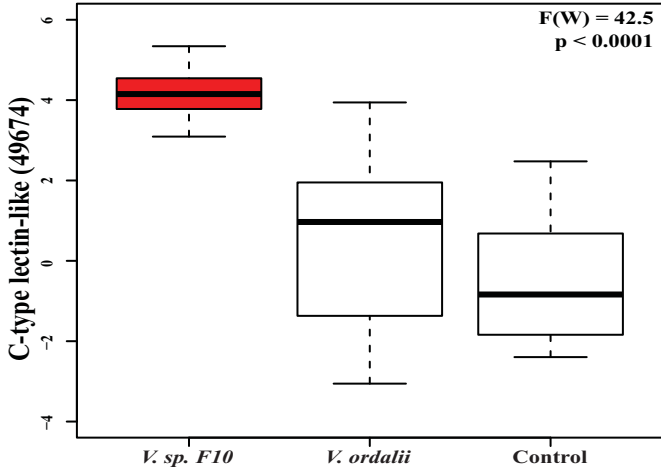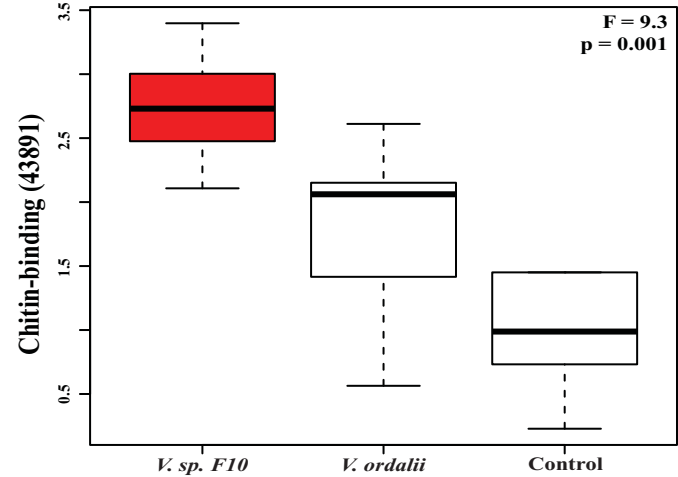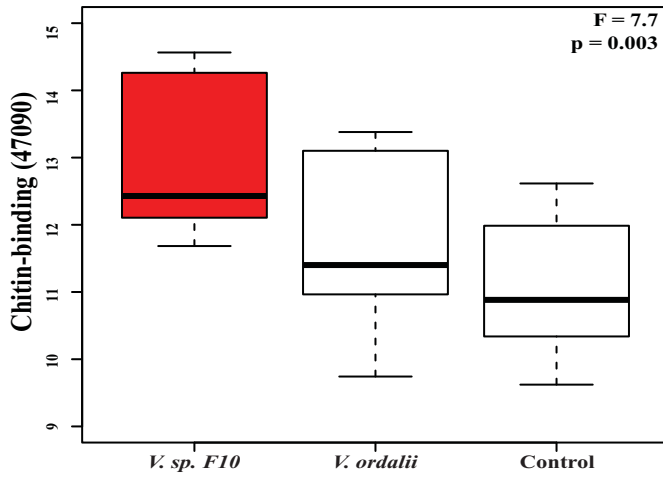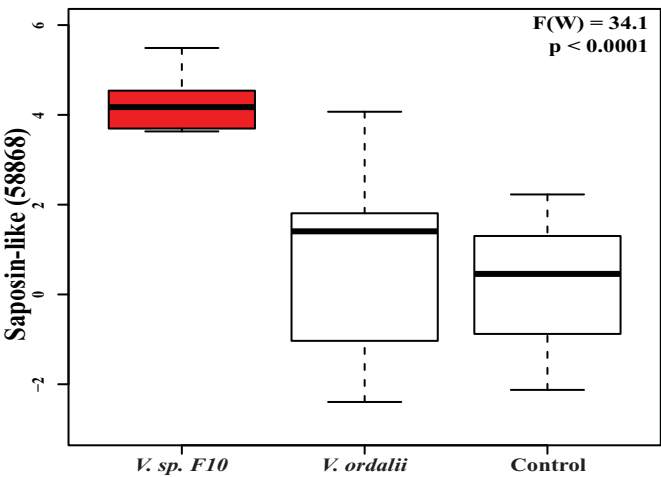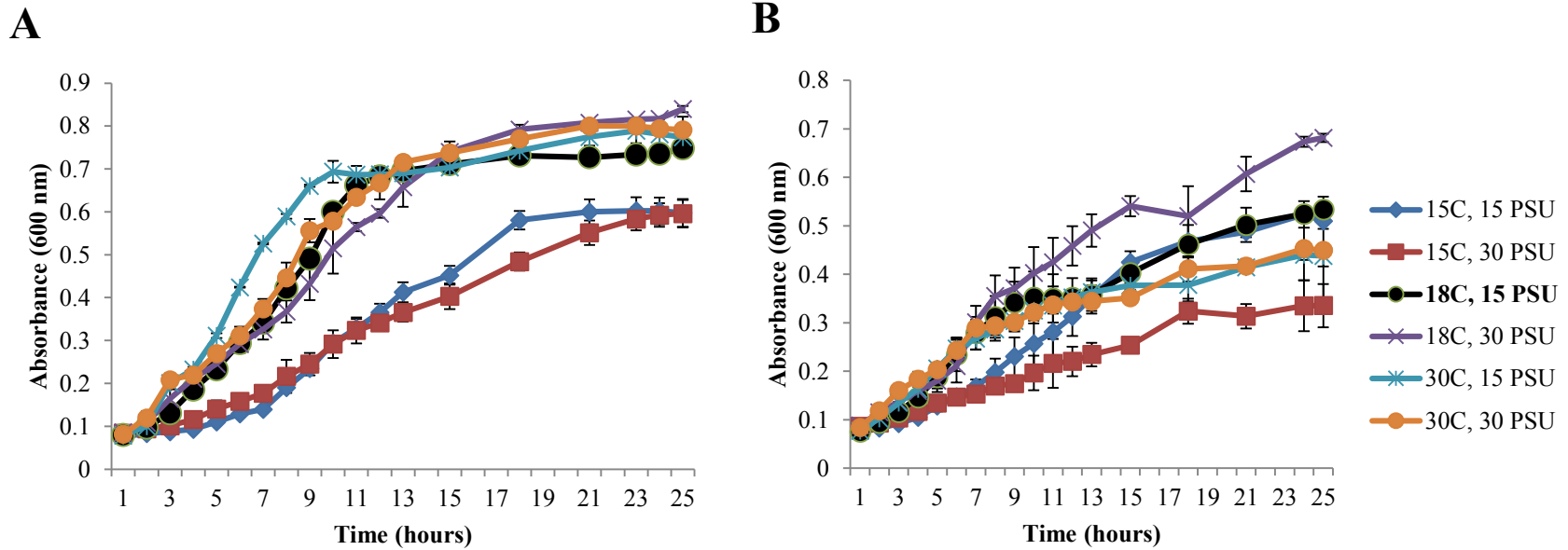
Figure S1: Growth curves of *Vibrio ordalii 12B09* (A) and *Vibrio sp. F10 9ZB36* (B) in seawater complete media (SWC) at different salinities (15 and 30 PSU) and temperatures (15 °C, 18 °C, 30 °C). The conditions represented in bold font and by black circles (18 °C, 15 PSU) were those used in the *E. affinis-Vibrio* exposure experiments. The results represent the mean ± SE of two experiments run in triplicate wells.
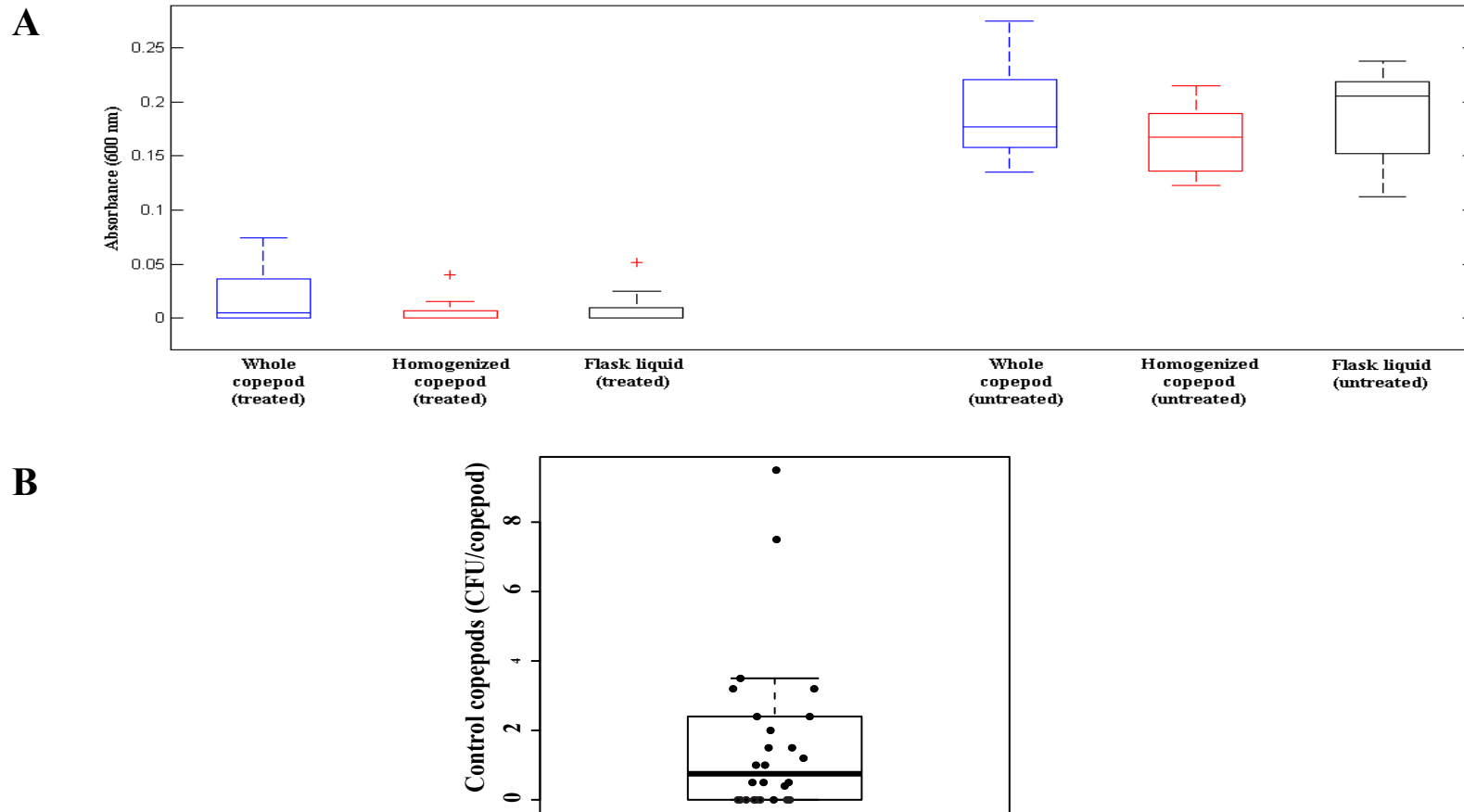
Figure S2: Validation of an antibiotic cocktail used to reduce the natural microbiota of *Eurytemora affinis*. Copepods were treated with a mixture of ampicillin (0.3 mg mL^{-1}), streptomycin (0.1 mg mL^{-1}), and chloramphenicol (0.05 mg mL^{-1}) for 24 hours. **A)** Individual whole copepods, homogenized copepods, or 400 μL of seawater from flasks containing either antibiotic treated or untreated copepods were placed into 2 mL of marine broth and the absorbance was measured after 48 hours of incubation at 22 °C. These boxplots represent 10 independent experiments. B) Plate count results of antiobiotic-treated, control, uninoculated copepod treatments at the end of the 24 hr Vibrio exposure experiments. Pools of copepods (n = 5 per replicate) were rinsed with artificial seawater, homogenized, and were either plated on seawater complete agar (15 PSU) or stained with DAPI. Direct counts were consistently so low as to be below the detection limit (<1 cell/field) and are not graphed here. Each circle represents the average number of colony forming units per copepod in 26 independent pooled samples.
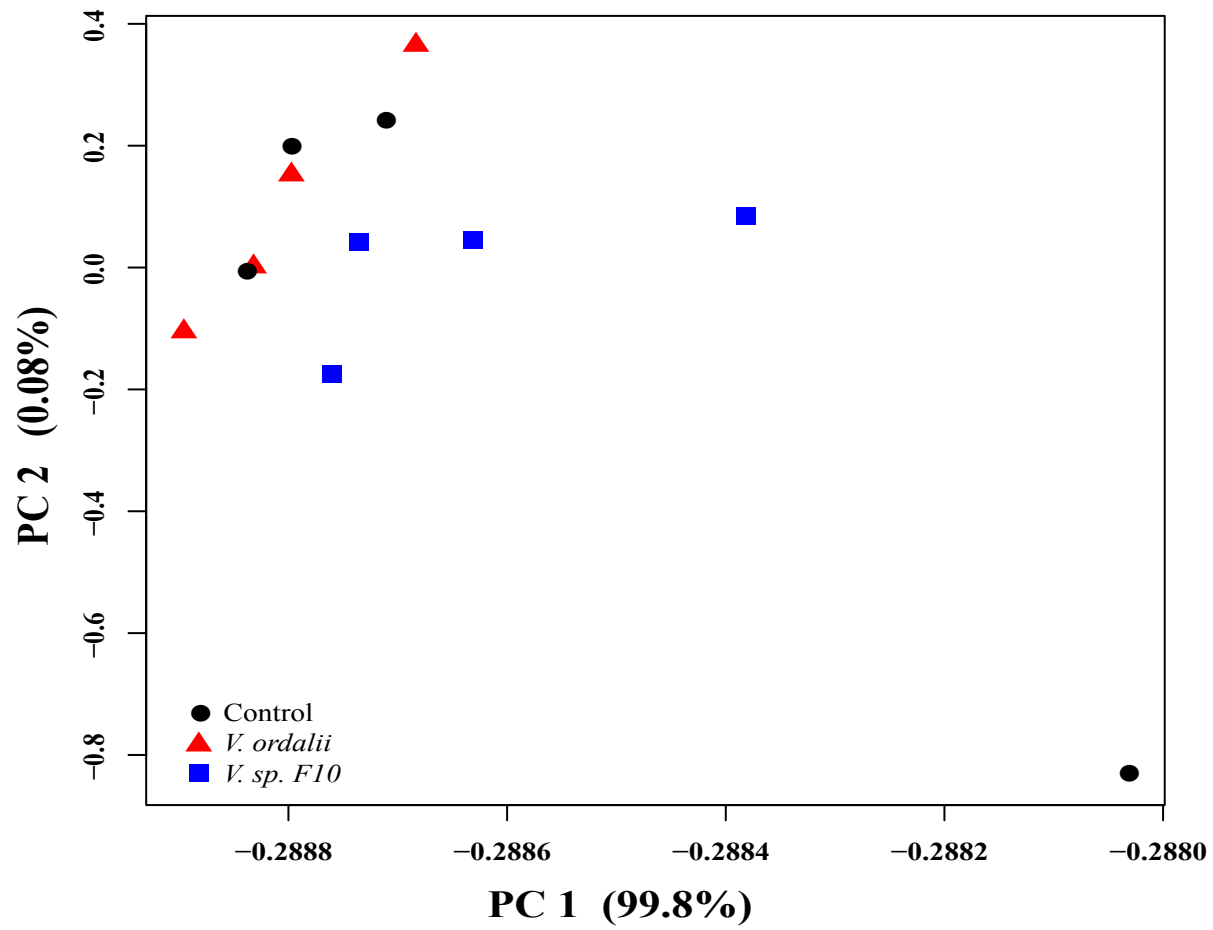
Figure S3: Principal component analysis of FPKM- and TMM-normalized Illumina gene expression data across all *Vibrio* samples suggests one biological replicate of the control treatment is an outlier. This biological replicate (plotted in black in the lower right hand corner) was subsequently dropped from further analysis.
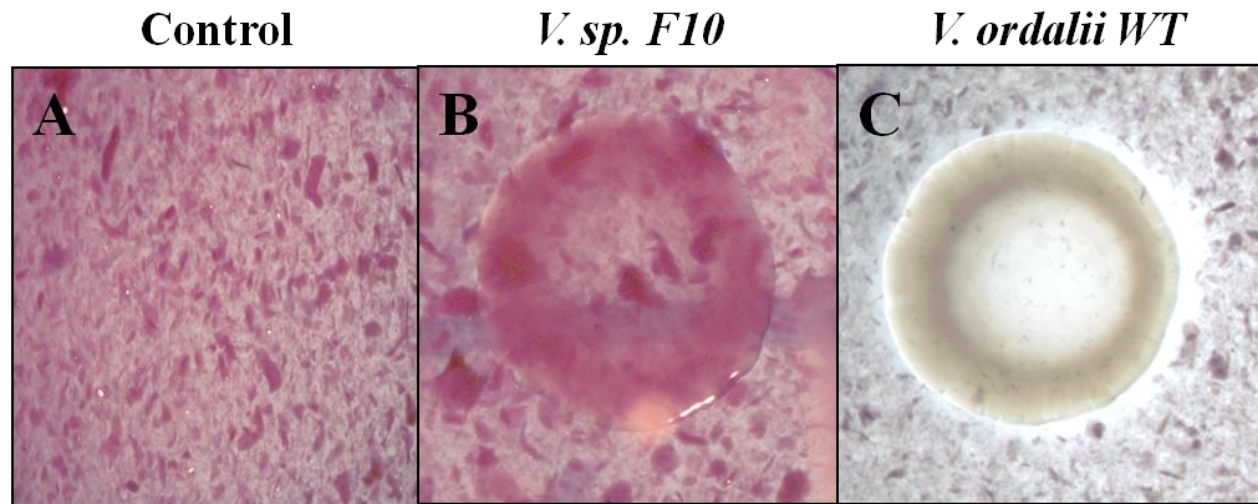
Figure S4: Exogeneous chitinase production of *Vibrio* strains was tested using a Remazol Brilliant Violet-labeled colloidal chitin agar plate. (A) The sterile plate control is purple due to the labeled chitin particles. *Vibrio* strains that do not produce exogeneous chitinase under the conditions examined will grow on the marine agar plate, but those *Vibrio* strains that secrete chitinases will grow and also produce a clear halo surrounding the colony due to the cleavage of the chitin particles and the Remzaol dye. Our results suggest that under the conditions examined *V. ordalii 12B09* (C) produces an exogeneous chitinase, while *V. sp. F10 9ZB36* does not (B).
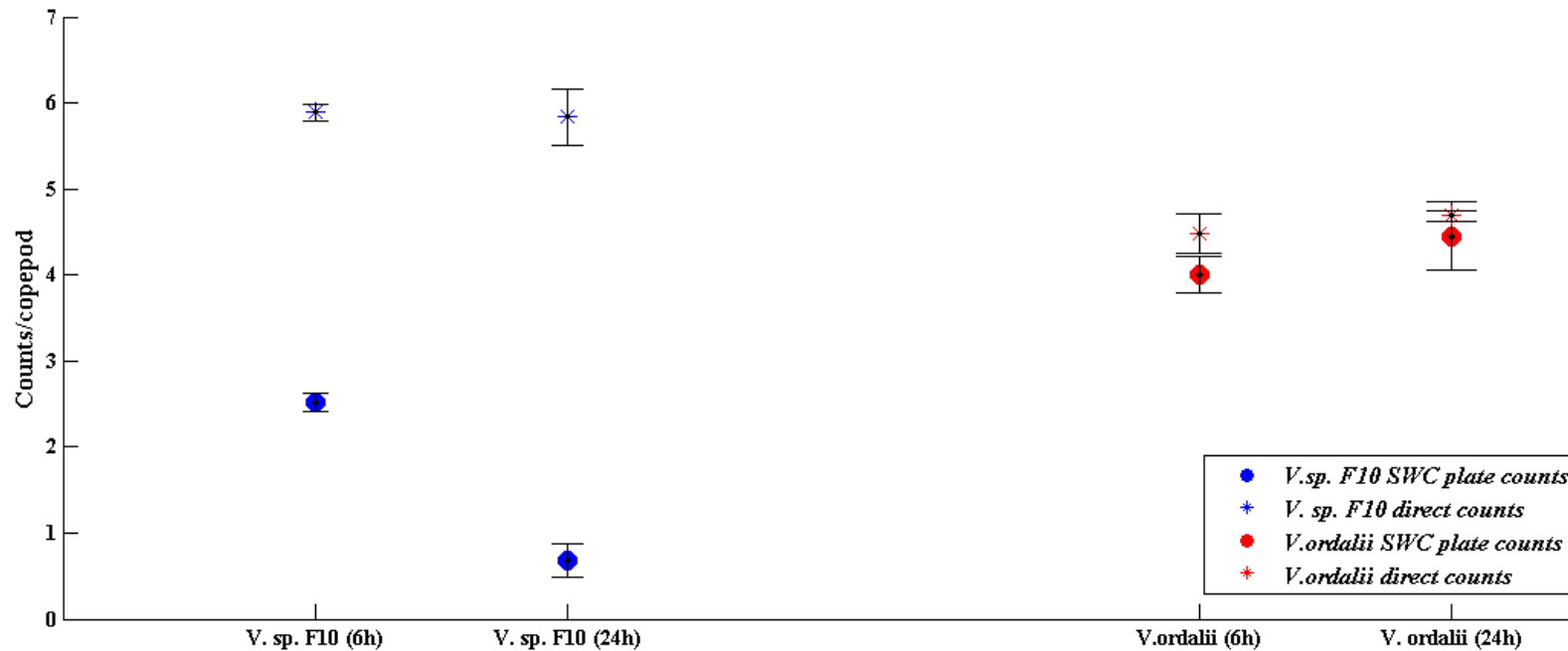
Figure S5: Association with the copepod *E. affinis* rapidly and specifically alters the culturability of *V. sp. F10*. After either 6 or 24 hour exposure to a *Vibrio* species, pools of copepods (n = 5 per replicate) were rinsed with artificial seawater, homogenized, and were either plated on seawater complete agar (15 PSU) (solid circles) or stained with DAPI (star symbol). Abundance counts are listed as the $\log_{10}$ of means ± 95% confidence interval of two biological replicates. All treatments had two biological replicates. Direct counts of control, uninoculated copepods were consistently so low as to be below the detection limit (< 1 cell/field).
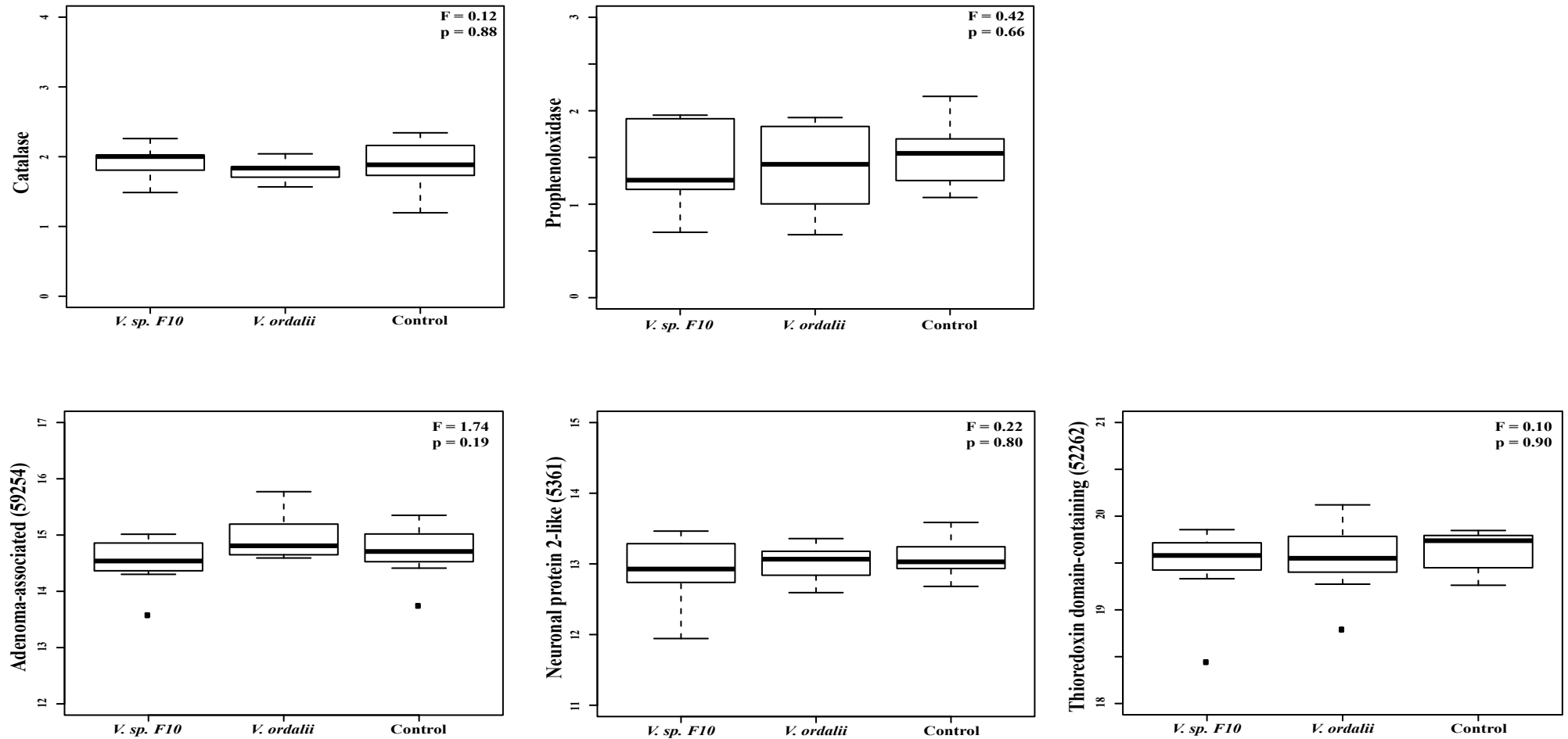
Figure S6: qPCR expression profiling of prophenoloxidase, catalse, and three housekeeping genes. Gene expression was measured in pooled samples of adult female *E. affinis* (n = 10-20 individuals) and results from three independent *Vibrio* exposure experiments were pooled for a total of n = 10, 9, 8 biological replicates in the control, *V. ordalii*, and *V. sp. F10* treatments, respectively. Prophenoloxidase and catalast expression values were normalized to housekeeping genes and base-2 log-transformed. The expression values of the three housekeeping genes are base-2 log-transformed for the boxplots shown above. One-way ANOVAs were not statistically significant (p > 0.05) for any of the plots shown.

Table S1: Comparison of the present study with recent studies utilizing next-generation sequencing technologies to assemble *de novo* transcriptomes of crustacean species.

Species	Description	Read length (bp)	Number of reads (million)	Contigs	'Genes'	N50	Contig length range	Platform	Assembler	Investigator
Eurytemora affinis	Estuarine copepod	100	100	138,581	82,891	2,087	201-23,627	Illumina	Trinity	Almada (current study)
Calanus finmarchicus	Marine copepod	100	80	241,778	124,618	987	201-25,048	Illumina	Trinity	Tarrant *et al*. (2014) *Front Zool*
Calanus finmarchicus	Marine copepod	100	400	206,041	96,090	1,418	300-23,068	Illumina	Trinity	Lenz *et al*. (2014) *PLoS ONE*
Tigriopus californicus	Intertidal copepod	384	0.6	22,262	42,473	(925: mean contig length)	8807 (max)	454	CLC Genomics Workbench	Barreto *et al*. (2011) *Mol Ecol*
Parhyale hawaiensis	Amphipod	400	3	89,664	25,735	1,510	~60-8,000	454	Newbler	Zeng (2011) *BMC Genomics*
Calanus sinicus	Marine copepod	380	1.5	56,809	~14,000	873	~100-3,500	454	Newbler	Ning *et al*. (2013) *PLoS ONE*

Table S2: *E. affinis* **mortality rates after exposure to** *Vibrio* **at 18 °C, 15 PSU for 24 or 48 hours.**

Vibrio strain	Inoculation density (CFU mL^{-1})	Mortality (%)	Length of Exposure (h)
V. sp. F10 9ZB36	1 x 10^7	0 ± 0 [a]	24
V. sp. F10 9ZB36	2 x 10^7	0 ± 0 [a]	24
V. sp. F10 9ZB36	2.5 x 10^7	0 ± 0 [a]	24
V. sp. F10 9ZB36	6 x 10^7	0 ± 0 [a]	24
V. ordalii 12B09	6 x 10^6	0 ± 0	24
V. ordalii 12B09	6 x 10^6	0 ± 0	48
V. ordalii 12B09	7 x 10^6	5 ± 5	24
V. ordalii 12B09	2 x10^7	0 ± 0	24
V. ordalii 12B09	3 x 10^7	10 ± 10 [a]	24
V. ordalii 12B09	6 x 10^7	0 ± 0	24
V. ordalii 12B09	6 x 10^7	0 ± 0	24
V. ordalii 12B09	6 x 10^7	5 ± 5	48
V. ordalii 12B09	7 x 10^7	5 ± 5	24

[a] indicates that 2 replicates of n = 5 individuals were tested. All other treatments tested 2 replicates of n = 10 individuals

Table S3: *E. affinis* genes differentially expressed in the *V. sp. F10* exposure treatment, compared to the control samples.
Abbreviations: 'FC' = fold change relative to the control treatment; 'FDR' = false discovery rate; 'GOs' = gene ontology terms. Blank entries reflect a lack of significant blast hits with associated GO terms at the set parameters (E-value < 1 x 10^{-4}). Positive and negative FC values reflect genes up-regulated and down-regulated, respectively, in the *V. sp. F10*-exposed treatment compared to the control treatment. Differentially expressed genes that were further profiled via qPCR are in bold. Genes indicated with '#' are those that are differentially expressed in both *Vibrio* exposure treatments in comparison to the control samples (comp51822_c0, comp40339_c0).

Transcript Description	Transcript ID	FC	FDR	Top BLASTx Hit Species	Top Hit Accession Number	Min. E-Value	Mean similarity	GOs	InterProScan results
CELL SIGNALLING PROCESSES									
homeobox protein nkx	comp12937_c0	-3.18	3.34E-02	*Strongyloides ratti* (nematode)	CEF65008	1.50E-05	47.00%	F:DNA binding	IPR001356 (homeobox domain); IPR009057 (homeodomain-like domain)
a disintegrin and metalloproteinase with thrombospondin motifs partial	comp42146_c0	1.87	2.21E-02	*Stegodyphus mimosarum* (spider)	KFM61983	6.86E-73	72.00%	P:proteolysis; F:metalloendopeptidase activity	IPR001590 (peptidase_M12B domain); IPR024079 (metallopeptidase catalytic domain)
f-box kelch-repeat protein at2g44130-like	comp42229_c0	1.16	3.68E-08	*Pyrus x bretschneideri* (pear)	XP_009335865	1.28E-06	46.67%	-	signal peptide domain; transmembrane domain
cholesterol desaturase daf-36-like	comp36258_c0	1.80	4.63E-06	*Latimeria chalumnae* (coelacanth)	XP_006009329	6.46E-104	61.33%	F:2 iron, 2 sulfur cluster binding; F:oxidoreductase activity; P:oxidation-reduction process	IPR017941 (Rieske [2Fe-2S] iron-sulphur domain); PTHR21266 (iron-sulfur domain containing); transmembrane helix domain
phosphatidylethanolamine-binding protein	comp48058_c1	-1.26	9.38E-05	*Danaus plexippus* (butterfly)	EHJ71177	8.45E-18	47.67%	-	IPR008914, PTHR11362 (phosphatidylethanolamine-binding protein PEBP family); cytoplasmic domain; transmembrane helix domain
beta-crystallin a1	comp51193_c0	1.29	9.21E-15	*Lepeophtheirus salmonis* (copepod)	ADD38111	1.21E-35	54.33%	-	IPR001064 (Beta/gamma crystallin); signal peptide domain ; IPR011024 (Gamma-crystallin-related domain)
hypothetical protein	comp57629_c1	1.16	2.78E-05	*Daphnia pulex* (waterflea)	EFX79782	7.28E-91	39.67%	F:serine-type endopeptidase inhibitor activity	SSF54403 (cystatin/monellin family); IPR002223 (Proteinase inhibitor I2, Kunitz domain); IPR018073 (Proteinase inhibitor I25, cystatin, conserved site); signal peptide domain

METABOLISM									
hypothetical protein	comp45348_c0	-3.36	6.21E-09	*Ciona intestinalis* (tunicate)	XP_002121160	4.00E-42	56.33%	-	PTHR10366 (NAD dependent epimerase/dehydratase); IPR027417 (P-loop containing nucleoside triphosphate hydrolase); transmembrane helix domain
violaxanthin de-epoxidase	comp42733_c0	1.38	4.73E-14	*Physcomitrella patens* (moss)	XP_001773358	5.55E-13	40.00%	F:violaxanthin de-epoxidase activity; C:chloroplast; P:oxidation-reduction process	IPR012674 (calycin domain); IPR010788 (violaxanthin de-epoxidase) ; IPR011038 (calycin-like superfamily); signal peptide domain
hypothetical protein	comp53782_c0	1.12	5.86E-05	*Daphnia pulex* (waterflea)	EFX83386	1.13E-92	55.00%	F:hydrolase activity	IPR002018, IPR019826 (carboxylesterase, type B domain/active site); IPR029058 (alpha/Beta hydrolase fold domain); PTHR11559 (carboxylesterase family); signal peptide domain
aldehyde dehydrogenase family 3 member partial	comp56580_c0	-1.00	6.01E-04	*Stegodyphus mimosarum* (spider)	KFM66996	3.36E-175	69.33%	F:oxidoreductase activity; P:biological_process	IPR012394, PTHR11699 (Aldehyde dehydrogenase NAD(P)-dependent family); IPR016162 (Aldehyde dehydrogenase, N-terminal domain); IPR016163 (Aldehyde dehydrogenase, C-terminal domain); cytoplasmic domain; transmembrane domain
aldehyde oxidase 2-like	comp59156_c0	-1.07	3.99E-04	*Daphnia pulex* (waterflea)	EFX86357	0.00E+00	60.67%	F:molecular_function	IPR005107 (CO dehydrogenase flavoprotein, C-terminal domain); IPR000674 (aldehyde oxidase/xanthine dehydrogenase, a/b hammerhead domain); IPR016208 (Aldehyde oxidase/xanthine dehydrogenase family); IPR008274 (Aldehyde oxidase/xanthine dehydrogenase, molybdopterin binding domain)

RESPONSE TO STRESS									
inter-alpha-trypsin inhibitor heavy chain h4	comp32809_c1	1.59	1.53E-04	*Crassostrea gigas* (oyster)	EKC36390	6.50E-102	55.67%	-	no IPS match
Cytochrome P450	comp55690_c0	-1.50	2.38E-03	*Tigriopus japonicus* (copepod)	AIL94133	1.16E-87	53.67%	P:oxidation-reduction process; F:iron ion binding; F:oxidoreductase activity, acting on paired donors, with incorporation or reduction of molecular oxygen; F:heme binding	IPR001128 (cytochrome P450 family); IPR002401 (cytochrome P450, E-class, group I family); signal peptide domain
glutathione s-transferase mu 1	comp46208_c1	-1.04	4.77E-03	*Oryctolagus cuniculus* (rabbit)	NP_001075721	2.87E-37	51.33%	F:protein binding	IPR004046 (Glutathione S-transferase, C-terminal domain); IPR004045 (Glutathione S-transferase, N-terminal domain); IPR010987 (glutathione S-transferase, C-terminal-like domain)
CUTICLE INTEGRITY									
chitotriosidase	comp55805_c0	1.28	6.34E-11	*Daphnia pulex* (waterflea)	EFX90412	2.17E-134	66.00%	F:hydrolase activity, acting on glycosyl bonds; P:biological_process	IPR017853 (glycoside hydrolase, superfamily); IPR011583 (chitinase II domain); IPR002557 (chitin-binding domain); IPR029070 (chitinase insertion domain); PTHR11177 (chitinase family); signal peptide domain
chondroitin proteoglycan-2-like	comp35157_c0	1.88	4.63E-06	*Tribolium castaneum* (beetle)	XP_008192409	4.01E-08	60.33%	C:extracellular region; P:chitin metabolic process; F:chitin binding	IPR002557 (chitin-binding domain); PTHR23301 (chitin-binding peritrophin A family)
chitin-binding protein	**comp43891_c0**	**2.10**	**3.42E-11**	***Drosophila virilis* (fly)**	**XP_002048076**	**3.65E-05**	**57.67%**	**P:chitin metabolic process; C:extracellular region; F:chitin binding**	**chitin-binding domain (PFAM); signal peptide domain**
chondroitin proteoglycan-2-like	**comp47090_c0**	**2.03**	**5.71E-10**	***Tribolium castaneum* (beetle)**	**XP_008192409**	**1.86E-09**	**60.33%**	**F:chitin binding; P:chitin metabolic process; C:extracellular region**	**IPR002557 (chitin-binding domain)**

IMMUNE SYSTEM PROCESSES									
C-type lectin-like	**comp47544_c0**	**4.61**	**2.55E-28**	-	-	-	-	-	**IPR016186 (c-type lectin-like domain); IPR016187 (c-type lectin fold domain); signal peptide domain**
macrophage mannose receptor partial	comp50187_c1	-1.80	8.02E-04	*Chaetura pelagica* (bird)	KFU96626	1.50E-15	41.67%	F:carbohydrate binding	IPR001304 (c-type lectin domain); PTHR22803 (mannose, phospholipase, lectin receptor related family); IPR016187 (c-type lectin fold domain); signal peptide domain
hepatic lectin-like	**comp49674_c0**	**6.93**	**4.15E-49**	***Oreochromis niloticus* (fish)**	**XP_005459156**	**3.02E-05**	**37**	**F:carbohydrate binding**	**IPR001304 (c-type lectin domain); IPR016186 (c-type lectin-like domain); IPR016187 (c-type lectin fold); cytoplasmic domain; transmembrane helix domain**
C-type lectin-like	comp46353_c0	8.21	3.99E-14	-	-	-	-	-	IPR016186 (c-type lectin-like domain); IPR016187 (c-type lectin fold)
C-type lectin-like	**comp46353_c1**	**7.64**	**6.90E-45**	-	-	-	-	-	**IPR016186 (c-type lectin-like domain); IPR016187 (c-type lectin fold)**
C-type lectin-like	comp40027_c0	5.99	3.99E-14	-	-	-	-	-	IPR016186 (c-type lectin-like); IPR016187 (c-type lectin fold)
c-type mannose receptor 2- partial	comp43463_c0	-1.16	1.41E-02	*Saccoglossus kowalevskii* (worm)	XP_006825556	2.63E-18	44.67%	F:carbohydrate binding	IPR001304 (c-type lectin); IPR016186 (c-type lectin-like); PTHR22803 (mannose, phospholipase, lectin receptor related); IPR016187 (c-type lectin fold); signal peptide domain
Saposin-like	**comp58868_c1**	**4.52**	**2.49E-73**	-	-	-	-	-	**IPR011001 (saposin-like domain); IPR008139 (saposin B domain); signal peptide domain**

TRANSPORT								
sodium-dependent phosphate transporter 1-a-like	comp51144_c0	1.12	3.86E-03	*Metaseiulus occidentalis* (mite)	XP_003742817	1.38E-67	52.67%	F:inorganic phosphate transmembrane transporter activity; C:membrane; P:phosphate ion transport	IPR001204 (phosphate transporter family); cytoplasmic domain; transmembrane helix domain
peptide transporter family 1-like	comp56914_c0	1.64	2.73E-07	*Dendroctonus ponderosae* (beetle)	ENN73556	3.13E-159	59.33%	F:transporter activity; C:membrane; P:oligopeptide transport	IPR000109 (Proton-dependent oligopeptide transporter family); PTHR11654:SF96 (peptide transporter family 1); IPR018456 (PTR2 family proton/oligopeptide symporter, conserved site); IPR016196 (Major facilitator superfamily domain, general substrate transporter domain); transmembrane helix domain; cytoplasmic domain
hypothetical protein	comp57280_c0	1.04	1.96E-05	*Daphnia pulex* (waterflea)	EFX71591	1.72E-149	52.00%	-	IPR002035 (von Willebrand factor, type A domain); IPR013642 (Chloride channel calcium-activated); PTHR10579 (calcium-activated chlorine channel regulator); cytoplasmic domain; transmembrane domain
adp-ribosylation factor	comp45127_c0	2.03	2.68E-05	*Dugesia japonica* (flatworm)	P91924	1.69E-71	82.33%	P:response to stress; P:catabolic process; P:signal transduction; P:vesicle-mediated transport; P:transport; C:Golgi apparatus; F:ion binding	IPR006689 (Small GTPase superfamily, ARF/SAR type); IPR027417 (P-loop containing nucleoside triphosphate hydrolase domain); IPR005225 (Small GTP-binding protein domain)

UNKNOWN									
Unknown	comp62318_c0	2.83	3.06E-02	-	-	-	-	-	signal peptide domain
Unknown	comp16598_c0	2.65	2.13E-02	-	-	-	-	-	transmembrane helix domain; cytoplasmic domain
Unknown	comp16910_c0	4.16	2.58E-08	-	-	-	-	-	no IPS match
Unknown	comp17377_c0	2.48	1.09E-03	-	-	-	-	-	G3DSA:3.50.4.10 (hepatocyte growth factor superfamily); signal peptide domain
Unknown	comp17945_c0	1.24	3.75E-10	-	-	-	-	-	G3DSA:3.50.4.10 (hepatocyte growth factor superfamily); signal peptide domain
hypothetical protein	comp18829_c0	1.90	1.49E-08	*Helobdella robusta* (leech)	XP_009029394	8.92E-04	44.00%	-	signal peptide domain
Unknown	comp58868_c2	4.00	9.54E-12	-	-	-	-	-	no IPS match
Unknown	comp58868_c3	4.07	5.23E-19	-	-	-	-	-	no IPS match
Unknown	comp56716_c0	1.26	2.04E-02	-	-	-	-	-	no IPS match
Unknown#	comp51822_c0	-5.53	6.05E-03	-	-	-	-	-	transmembrane helix domain
Unknown	comp52925_c1	2.50	4.15E-49	-	-	-	-	-	G3DSA:3.50.4.10 (hepatocyte growth factor superfamily); signal peptide domain
Unknown	comp53341_c1	1.67	4.97E-02	-	-	-	-	-	IPR029469 (PAN-4 domain); G3DSA:3.50.4.10 (hepatocyte growth factor superfamily); signal peptide domain
Unknown	comp53341_c2	1.64	3.86E-03	-	-	-	-	-	IPR029469 (PAN-4 domain); G3DSA:3.50.4.10 (hepatocyte growth factor superfamily); signal peptide domain
Unknown	comp53492_c0	1.76	1.89E-02	-	-	-	-	-	cytoplasmic domain; transmembrane helix domain
Unknown	comp49776_c0	-6.42	3.61E-03	-	-	-	-	-	no IPS match
Unknown	comp50150_c0	1.08	4.43E-02	-	-	-	-	-	coiled-coil domain; transmembrane domain

Unknown	comp46444_c2	2.83	3.53E-04	-	-	-	-	-	signal peptide domain
Unknown	comp46722_c0	2.46	5.94E-04	-	-	-	-	-	no transmembrane domain
Unknown	comp47218_c0	1.06	3.34E-02	-	-	-	-	-	signal peptide domain; transmembrane helix domain
Unknown	comp46043_c0	2.93	3.99E-04	-	-	-	-	-	no IPS match
Unknown	comp44011_c0	3.11	9.29E-07	-	-	-	-	-	no IPS match
Unknown#	comp40339_c0	-8.35	3.53E-04	-	-	-	-	-	signal peptide domain; transmembrane domain
Unknown	comp40368_c0	1.99	4.09E-06	-	-	-	-	-	G3DSA:3.50.4.10 (hepatocyte growth factor superfamily); SSF57414 (hairpin loop containing domain-like superfamily)
Unknown	comp41942_c0	1.99	2.82E-12	-	-	-	-	-	no IPS match
Unknown	comp42970_c0	-4.86	4.83E-02	-	-	-	-	-	transmembrane domain
Unknown	comp43319_c0	2.19	1.33E-06	-	-	-	-	-	IPR003014 (PAN-1 domain); IPR003609 (apple-like domain) SSF57414 (hairpin loop containing domain-like superfamily); signal peptide domain
Unknown	comp33114_c0	-4.03	2.31E-03	-	-	-	-	-	no IPS match
Unknown	comp36118_c0	1.31	5.91E-06	-	-	-	-	-	G3DSA:3.50.4.10 (hepatocyte growth factor superfamily); signal peptide domain
Unknown	comp36128_c0	1.86	6.66E-04	-	-	-	-	-	transmembrane, cytoplasmic domain
Unknown	comp39845_c0	3.38	1.48E-02	-	-	-	-	-	no IPS match

Table S4: *E. affinis* genes differentially expressed in the *V. ordalii* exposure treatment, compared to the control samples.
Abbreviations: 'FC' = fold change relative to the control treatment; 'FDR' = false discovery rate; 'GOs' = gene ontology terms. Blank entries reflect a lack of significant blast hits with associated GO terms at the set parameters (E-value $< 1 \times 10^{-4}$). Positive and negative FC values reflect genes up-regulated and down-regulated, respectively, in the *V. ordalii*-exposed treatment compared to the control treatment. Genes indicated with '#' are those that are differentially expressed in both *Vibrio* exposure treatments in comparison to the control samples (comp51822_c0, comp40339_c0).

Transcript Description	Transcript ID	FC	FDR	Top BLASTx Hit Species	Top Hit Accession Number	Min. E-Value	Mean similarity	GOs	InterProScan results
RESPONSE TO STRESS									
Knottin-like inhibitory protein	comp44575_c0	-2.81	2.86E-03	-	-	-	-	P:defense response	IPR003614 (knottin, scorpion-toxin-like domain); signal peptide domain
UNKNOWN									
Unknown#	comp40339_c0	-7.66	1.17E-02	-	-	-	-	-	signal peptide domain; transmembrane domain
Unknown#	comp51822_c0	-5.90	1.17E-02	-	-	-	-	-	transmembrane helix domain

Table S5: *E. affinis* genes differentially expressed in the *V. ordalii* exposure treatment, compared to the *V. sp. F10* exposure treatment. Abbreviations: 'FC' = fold change relative to the control treatment; 'FDR' = false discovery rate; 'GOs' = gene ontology terms. Blank entries reflect a lack of significant blast hits with associated GO terms at the set parameters (E-value < 1 x 10⁻⁴). Positive and negative FC values reflect genes up-regulated and down-regulated, respectively, in the *V. ordalii*-exposed treatment compared to the *V. sp. F10*-exposed treatment. Genes that are uniquely differentially expressed in the comparison of the *Vibrio* exposure treatments are indicated in bold.

Transcript Description	Transcript ID	FC	FDR	Top BLASTx Hit Species	Top Hit Accession Number	Min. E-Value	Mean similarity	GOs	InterProScan results
CELL SIGNALLING PROCESSES									
beta-crystallin a1	**comp45441_c0**	**-1.14**	**1.76E-02**	*Lepeophtheirus salmonis* (copepod)	**ADD38111**	**8.62E-37**	**54.33%**	**-**	**G3DSA:2.60.20.10 (crystallin superfamily); IPR011024 (gamma-crystallin related domain); IPR001064 (Beta/gamma crystallin domain)**
a disintegrin and metalloproteinase with thrombospondin motifs partial	comp42146_c0	-1.36	9.78E-02	*Stegodyphus mimosarum* (spider)	KFM61983	6.86E-73	72.00%	P:proteolysis; F:metalloendopeptidase activity	IPR001590 (peptidase_M12B domain); IPR024079 (metallopeptidase catalytic domain)
f-box kelch-repeat protein at2g44130-like	comp42229_c0	-1.07	8.22E-06	*Pyrus x bretschneideri* (pear)	XP_009335865	1.28E-06	46.67%	-	signal peptide domain; transmembrane domain
f-box kelch-repeat protein at2g44130-like	**comp21522_c0**	**-1.30**	**8.33E-03**	***Pyrus x bretschneideri* (pear)**	**XP_009335865**	**4.15E-07**	**46.33%**	**F:protein binding**	**SSF117281 (kelch motif superfamily); IPR006652 (kelch repeat type 1); IPR015915 (kelch-type beta propeller domain)**
elongation factor 1-delta	**comp45173_c0**	**-2.97**	**4.22E-02**	***Artemia salina* (brine shrimp)**	**P32192**	**9.88E-26**	**65.00%**	**C:eukaryotic translation elongation factor 1 complex; P:translational elongation; F:translation elongation factor activity**	**IPR014038 (translation elongation factor EF1B, beta/delta subunit, guanine nucleotide exchange domain)**
beta-crystallin a1	comp51193_c0	-1.15	7.31E-12	*Lepeophtheirus salmonis* (copepod)	ADD38111	1.21E-35	54.33%	-	IPR001064 (Beta/gamma crystallin); signal peptide domain ; IPR011024 (Gamma-crystallin-related domain)

METABOLISM									
hypothetical protein	comp45348_c0	3.10	4.76E-13	*Ciona intestinalis* (tunicate)	XP_002121160	4.00E-42	56.33%	-	PTHR10366 (NAD dependent epimerase/dehydratase); IPR027417 (P-loop containing nucleoside triphosphate hydrolase); transmembrane helix domain
violaxanthin de-epoxidase	comp42733_c0	-1.26	4.46E-10	*Physcomitrella patens* (moss)	XP_001773358	5.55E-13	40.00%	F:violaxanthin de-epoxidase activity; C:chloroplast; P:oxidation-reduction process	IPR012674 (calycin domain); IPR010788 (violaxanthin de-epoxidase) ; IPR011038 (calycin-like superfamily); signal peptide domain
hypothetical protein	comp53782_c0	-0.96	3.65E-03	*Daphnia pulex* (waterflea)	EFX83386	1.13E-92	55.00%	F:hydrolase activity	IPR002018, IPR019826 (carboxylesterase, type B domain/active site); IPR029058 (alpha/Beta hydrolase fold domain); PTHR11559 (carboxylesterase family); signal peptide domain
aldehyde dehydrogenase family 3 member partial	comp56580_c0	0.82	9.10E-02	*Stegodyphus mimosarum* (spider)	KFM66996	3.36E-175	69.33%	F:oxidoreductase activity; P:biological_process	IPR012394, PTHR11699 (Aldehyde dehydrogenase NAD(P)-dependent family); IPR016162 (Aldehyde dehydrogenase, N-terminal domain); IPR016163 (Aldehyde dehydrogenase, C-terminal domain); cytoplasmic domain; transmembrane domain
aldehyde oxidase 2-like	comp59156_c0	-4.14	5.26E-25	*Daphnia pulex* (waterflea)	EFX86357	0.00E+00	60.67%	F:molecular_function	IPR005107 (CO dehydrogenase flavoprotein, C-terminal domain); IPR000674 (aldehyde oxidase/xanthine dehydrogenase, a/b hammerhead domain); IPR016208 (Aldehyde oxidase/xanthine dehydrogenase family); IPR008274 (Aldehyde oxidase/xanthine dehydrogenase, molybdopterin binding domain)

RESPONSE TO STRESS									
Knottin-like inhibitory protein	comp44575_c0	-3.54	2.77E-02	-	-	-	-	P:defense response	IPR003614 (knottin, scorpion-toxin-like domain); signal peptide domain
inter-alpha-trypsin inhibitor heavy chain h4	comp32809_c1	-1.34	1.12E-02	*Crassostrea gigas* (oyster)	EKC36390	6.50E-102	55.67%	-	no IPS match
Cytochrome P450	comp55690_c0	1.67	4.54E-05	*Tigriopus japonicus* (copepod)	AIL94133	1.16E-87	53.67%	P:oxidation-reduction process; F:iron ion binding; F:oxidoreductase activity, acting on paired donors, with incorporation or reduction of molecular oxygen; F:heme binding	IPR001128 (cytochrome P450 family); IPR002401 (cytochrome P450, E-class, group I family); signal peptide domain
glutathione s-transferase mu 1	comp46208_c1	0.90	4.84E-02	*Oryctolagus cuniculus* (rabbit)	NP_001075721	2.87E-37	51.33%	F:protein binding	IPR004046 (Glutathione S-transferase, C-terminal domain); IPR004045 (Glutathione S-transferase, N-terminal domain); IPR010987 (glutathione S-transferase, C-terminal-like domain)
CUTICLE INTEGRITY									
Chitotriosidase	**comp33461_c0**	**-1.30**	**3.23E-04**	***Daphnia pulex* (waterflea)**	**EFX90412**	**8.52E-80**	**73.33%**	**F:hydrolase activity, acting on glycosyl bonds; P:biological_process; P:carbohydrate metabolic process**	**IPR017853 (Glycoside hydrolase, superfamily); PTHR11177 (chitinase family); IPR011583 (chitinase II domain); IPR001579 (Glycoside hydrolase, chitinase active site); signal peptide domain**
hypothetical protein	**comp32479_c0**	**-1.58**	**1.25E-03**	***Daphnia pulex* (waterflea)**	**EFX90414**	**1.20E-45**	**63.33%**	**F:hydrolase activity, acting on glycosyl bonds; P:biological_process**	**IPR017853 (Glycoside hydrolase, superfamily domain); IPR001223 (Glycoside hydrolase, family 18, catalytic domain); IPR029070 (chitinase insertion domain); PTHR11177 (chitinase family)**
chitotriosidase	comp55805_c0	-1.29	2.82E-09	*Daphnia pulex* (waterflea)	EFX90412	2.17E-134	66.00%	F:hydrolase activity, acting on glycosyl bonds; P:biological_process	IPR017853 (glycoside hydrolase, superfamily); IPR011583 (chitinase II domain); IPR002557 (chitin-binding domain); IPR029070 (chitinase insertion domain); PTHR11177 (chitinase family); signal peptide domain
chondroitin proteoglycan-2-like	comp35157_c0	-1.60	4.70E-06	*Tribolium castaneum* (beetle)	XP_008192409	4.01E-08	60.33%	C:extracellular region; P:chitin metabolic process; F:chitin binding	IPR002557 (chitin-binding domain); PTHR23301 (chitin-binding peritrophin A family)

chitin-binding protein	comp43891_c0	-1.35	5.12E-06	*Drosophila virilis* (fly)	XP_002048076	3.65E-05	57.67%	P:chitin metabolic process; C:extracellular region; F:chitin binding	chitin-binding domain (PFAM); signal peptide domain
chondroitin proteoglycan-2-like	comp47090_c0	-1.96	6.08E-10	*Tribolium castaneum* (beetle)	XP_008192409	1.86E-09	60.33%	F:chitin binding; P:chitin metabolic process; C:extracellular region	IPR002557 (chitin-binding domain)
IMMUNE SYSTEM PROCESSES									
C-type lectin-like	comp47544_c0	-3.93	1.97E-20	-	-	-	-	-	IPR016186 (c-type lectin-like domain); IPR016187 (c-type lectin fold domain); signal peptide domain
macrophage mannose receptor partial	comp50187_c1	1.99	6.07E-05	*Chaetura pelagica* (bird)	KFU96626	1.50E-15	41.67%	F:carbohydrate binding	IPR001304 (c-type lectin domain); PTHR22803 (mannose, phospholipase, lectin receptor related family); IPR016187 (c-type lectin fold domain); signal peptide domain
hepatic lectin-like	comp49674_c0	-4.50	9.64E-08	*Oreochromis niloticus* (fish)	XP_005459156	3.02E-05	37	F:carbohydrate binding	IPR001304 (c-type lectin domain); IPR016186 (c-type lectin-like domain); IPR016187 (c-type lectin fold); cytoplasmic domain; transmembrane helix domain
C-type lectin-like	comp46353_c0	-4.98	2.64E-17	-	-	-	-	-	IPR016186 (c-type lectin-like domain); IPR016187 (c-type lectin fold)
C-type lectin-like	comp46353_c1	-5.04	2.82E-07	-	-	-	-	-	IPR016186 (c-type lectin-like domain); IPR016187 (c-type lectin fold)
C-type lectin-like	comp40027_c0	-3.53	1.33E-08	-	-	-	-	-	IPR016186 (c-type lectin-like); IPR016187 (c-type lectin fold)
c-type mannose receptor 2-partial	comp43463_c0	0.98	5.84E-02	*Saccoglossus kowalevskii* (worm)	XP_006825556	2.63E-18	44.67%	F:carbohydrate binding	IPR001304 (c-type lectin); IPR016186 (c-type lectin-like); PTHR22803 (mannose, phospholipase, lectin receptor related); IPR016187 (c-type lectin fold); signal peptide domain
Saposin-like	comp58868_c1	-3.76	1.03E-35	-	-	-	-	-	IPR011001 (saposin-like domain); IPR008139 (saposin B domain); signal peptide domain

TRANSPORT									
sodium-dependent phosphate transporter 1-a-like	comp51144_c0	-0.83	1.47E-01	*Metaseiulus occidentalis* (mite)	XP_003742817	1.38E-67	52.67%	F:inorganic phosphate transmembrane transporter activity; C:membrane; P:phosphate ion transport	IPR001204 (phosphate transporter family); cytoplasmic domain; transmembrane helix domain
sodium-dependent nutrient amino acid transporter 1-like	**comp12362_c0**	**-3.61**	**2.30E-02**	***Bombus terrestris* (bumblebee)**	**XP_003400703**	**2.47E-49**	**60.33%**	**P:neurotransmitter transport; F:neurotransmitter:sodium symporter activity; C:integral to membrane**	**IPR000175 (Sodium:neurotransmitter symporter family); SSF161070 (SNF-like superfamily); transmembrane helix domain; cytoplasmic domaiin**
peptide transporter family 1-like	comp56914_c0	-1.29	3.37E-04	*Dendroctonus ponderosae* (beetle)	ENN73556	3.13E-159	59.33%	F:transporter activity; C:membrane; P:oligopeptide transport	IPR000109 (Proton-dependent oligopeptide transporter family); PTHR11654:SF96 (peptide transporter family 1); IPR018456 (PTR2 family proton/oligopeptide symporter, conserved site); IPR016196 (Major facilitator superfamily domain, general substrate transporter domain); transmembrane helix domain; cytoplasmic domain
hypothetical protein	comp57280_c0	-0.92	6.55E-04	*Daphnia pulex* (waterflea)	EFX71591	1.72E-149	52.00%	-	IPR002035 (von Willebrand factor, type A domain); IPR013642 (Chloride channel calcium-activated); PTHR10579 (calcium-activated chlorine channel regulator); cytoplasmic domain; transmembrane domain
UNKNOWN									
Unknown	comp62318_c0	-3.06	2.01E-04	-	-	-	-	-	signal peptide domain
Unknown	comp16910_c0	-3.22	3.16E-10	-	-	-	-	-	no IPS match
Unknown	comp17945_c0	-1.25	3.84E-09	-	-	-	-	-	G3DSA:3.50.4.10 (hepatocyte growth factor superfamily); signal peptide domain
hypothetical protein	comp18829_c0	-1.85	8.61E-11	*Helobdella robusta* (leech)	XP_009029394	8.92E-04	44.00%	-	signal peptide domain

Unknown	comp58868_c2	-3.73	1.56E-16	-	-	-	-	-	no IPS match
Unknown	comp58868_c3	-4.14	5.26E-25	-	-	-	-	-	no IPS match
Unknown	comp56716_c0	-1.16	4.82E-01	-	-	-	-	-	no IPS match
Unknown	comp52925_c1	-2.18	2.85E-22	-	-	-	-	-	G3DSA:3.50.4.10 (hepatocyte growth factor superfamily); signal peptide domain
Unknown	comp53341_c1	-1.47	1.65E-01	-	-	-	-	-	IPR029469 (PAN-4 domain); G3DSA:3.50.4.10 (hepatocyte growth factor superfamily); signal peptide domain
Unknown	comp53341_c2	-1.47	2.96E-03	-	-	-	-	-	IPR029469 (PAN-4 domain); G3DSA:3.50.4.10 (hepatocyte growth factor superfamily); signal peptide domain
Unknown	comp53492_c0	-1.46	7.38E-02	-	-	-	-	-	cytoplasmic domain; transmembrane helix domain
Unknown	comp46444_c2	-2.99	8.67E-13	-	-	-	-	-	signal peptide domain
Unknown	comp46722_c0	-1.93	6.30E-04	-	-	-	-	-	no transmembrane domain
Unknown	comp46043_c0	-3.07	5.77E-08	-	-	-	-	-	no IPS match
Unknown	comp44011_c0	-2.49	2.18E-08	-	-	-	-	-	no IPS match
Unknown	comp40368_c0	-1.16	1.09E-02	-	-	-	-	-	G3DSA:3.50.4.10 (hepatocyte growth factor superfamily); SSF57414 (hairpin loop containing domain-like superfamily)
Unknown	comp41942_c0	-1.48	1.33E-07	-	-	-	-	-	no IPS match
Unknown	comp43319_c0	-1.95	3.69E-08	-	-	-	-	-	IPR003014 (PAN-1 domain); IPR003609 (apple-like domain) SSF57414 (hairpin loop containing domain-like superfamily); signal peptide domain

Unknown	comp36118_c0	-1.02	3.57E-03	-	-	-	-	-	G3DSA:3.50.4.10 (hepatocyte growth factor superfamily); signal peptide domain
Unknown	comp36128_c0	-2.07	2.75E-06	-	-	-	-	-	transmembrane, cytoplasmic domain
Unknown	comp39845_c0	-2.85	2.28E-03	-	-	-	-	-	no IPS match
Unknown	**comp73005_c0**	**-3.92**	**7.86E-03**	**-**	**-**	**-**	**-**	**-**	**no IPS match**
Unknown	**comp63041_c0**	**3.79**	**2.40E-02**	**-**	**-**	**-**	**-**	**-**	**coiled coil domain**
Unknown	**comp60209_c0**	**-1.39**	**4.23E-03**	**-**	**-**	**-**	**-**	**-**	**signal peptide domain**
Unknown	**comp57815_c2**	**1.41**	**2.74E-02**	**-**	**-**	**-**	**-**	**-**	**signal peptide domain; transmembrane helix domain**
Unknown	**comp48674_c0**	**-3.48**	**4.49E-02**	**-**	**-**	**-**	**-**	**-**	**no IPS match**
hypothetical protein	**comp43699_c0**	**8.02**	**3.92E-02**	***Acartia pacifica* (copepod)**	**AGN29688**	**9.37E-48**	**69.67%**	**-**	**no IPS match**
Unknown	**comp41891_c0**	**-3.40**	**2.30E-02**	**-**	**-**	**-**	**-**	**-**	**signal peptide domain**
Unknown	**comp40961_c0**	**-2.49**	**2.30E-02**	**-**	**-**	**-**	**-**	**-**	**transmembrane helix domain**
Unknown	**comp39791_c0**	**-2.42**	**3.85E-04**	**-**	**-**	**-**	**-**	**-**	**coiled-coil domain**
Unknown	**comp16303_c0**	**5.03**	**2.46E-02**	**-**	**-**	**-**	**-**	**-**	**signal peptide domain; transmembrane helix domain**

Table S6: Primer sequences and annealing temperatures used in cloning reactions.

Transcript name	Transcript ID		Primer sequence	T_a (°C)	Cloned sequence length (bp)
C-type lectin-like	comp47544_c0	F	CGGATGTGTTTCTGTTGAGCA	63	407
		R	TTGCTGCAAGTTGAGAGAGC		
C-type lectin	comp49674_c0	F	TCTTCATGGCCAGGAGAAGG	64	505
		R	TGCTACATCATTCCAGAGTCCA		
C-type lectin-like	comp46353_c1	F	AGCATTGGTTCTATTTCTGGAGA	63	417
		R	AGGAGCATTAATGGCCCAGT		
Chitin-binding	comp47090_c0	F	CATCTACACCCACCTACAATACTAC	62.2	298
		R	CTACAATTCTACATTTCAGCTGG		
Chitin-binding	comp43891_c0	F	GCTGTTCCTCTTAGTCTCTCTC	63	205
		R	GTAGAGAGGTGGAGCGCAG		
Catalase	comp50873_c0	F	GATGCCGCAAACTACTCACC	65.5	543
		R	CTGGTTTGGTTTGGTCCTGAG		
Prophenoloxidase	comp58098_c0	F	CTGCAATGCGTGATCCTCTC	65	790
		R	CTTCTCACTCCGCTGCTG		
Thioredoxin domain-containing protein	comp52622_c0	F	CAAGTTCTACGCTCCCTGG	65	689
		R	GAGTTCGTCCTTCTCTGCC		
Thyroid adenoma-associated protein homolog	comp59254_c0	F	CTGCCTGAAGAAGCTCACTC	65.5	735
		R	CTTGAAACCGTGTAGCCGAG		
Leucine-Rich Neuronal protein	comp53361_c0	F	CTACTGTACCTTGACCTCAGC	65.5	588
		R	CGTGACGTCATTGATCCAGG		
Saposin-like	comp58868_c1	F	TACCCCGTCTTCCTTGAACC	60.5	590
		R	TCCATGCAAAGGTACAACAGT		

Table S7: Primer sequences and annealing temperatures used in qPCR.

Transcript name	Transcript ID		Primer sequence	Ta (°C)
C-type lectin-like	comp47544_c0	F	CGGATGTGTTTCTGTTGAGC	62
		R	CCCTCCATTCCTTCATCAGTAG	
C-type lectin	comp49674_c0	F	CTGATGAAGGTATGGAGGGTC	63
		R	GCTAGCTGATATCCATGGGTG	
C-type lectin-like	comp46353_c1	F	AGCTGTCTGACCAACTCCTTAG	63
		R	GGTTCATCTTGTTCTGTCTTGC	
Chitin-binding	comp47090_c0	F	GCTACATCTACTTCACCATCCTAC	64
		R	CTGTACTTGGATGGCAAGCTAC	
Chitin-binding	comp43891_c0	F	GCTGTTCCTCTTAGTCTCTCTC	62
		R	ACAGTCAAATGGATGAGGAAC	
Catalase	comp50873_c0	F	ACAGGCTCGGACCTAACTTTG	64
		R	CTGGTTTGGTTTGGTCCTGAG	
Prophenoloxidase	comp58098_c0	F	CATCACCAAGTCTCCGCTTC	64
		R	GGTAGAACCATTGTCTCAGGC	
Thioredoxin domain-containing protein	comp52622_c0	F	GATTGTACCGAGCATCAGTCC	64
		R	GCTCATTCACCCAGTCCTTG	
Thyroid adenoma-associated protein homolog	comp59254_c0	F	ACCTAGGCTTGTCACTGAGC	64
		R	TGAAGAACAGTCCCTCTCCG	
Leucine-Rich Neuronal protein	comp53361_c0	F	TGACTGGTCCAAGCTCTCTG	64
		R	CGTGACGTCATTGATCCAGG	
Saposin-like	comp58868_c1	F	CGTCTTCCTTGAACCTGAGG	63
		R	CAGCTCCTGTACATTCTTCAC	

REFERENCES FOR SUPPORTING FIGURES AND TABLES:

Barreto FS, Moy GW, Burton RS (2011) Interpopulation patterns of divergence and selection across the transcriptome of the copepod *Tigriopus californicus*. Mol Ecol 3:560-5762.

Ning J, Wang M, Li C, Song S (2013) Transcriptome sequencing and do novo analysis of the copepod *Calanus sinicus* using 454 GS FLX. PLoS ONE (5):e63741.

Tarrant AM, Baumgartner MF, Hansen BH, Altin D, Nordtug T, Olsen AJ (2014) Transcriptional profiling of reproductive development, lipid storage and molting throughout the last juvenile stage of the marine copepod *Calanus finmarchicus*. Front Zool 11:91.

Zeng V, Villanueva KE, Ewen-Campben BS, Alwes F, Browne WE, Extavour CG (2011) De novo assembly and characterization of a maternal and developmental transcriptome for the emerging model crustacean *Parhyale hawiensis*. BMC Genomics 12:581.